



Water Resources Research

RESEARCH ARTICLE

10.1002/2017WR020651

Key Points:

- A dynamic model for assessing water-driven rangeland soil erosion rates is presented and tested
- Application of the model to a small, hillslope-sized watershed in SE Arizona showed improved predictive function over the previous steady state model for rangelands
- A case study of application of the model to 124 rangeland sites in the western United States illustrated the possibilities for using the model for broad-scale assessments

Correspondence to:

M. Hernandez,
Mariano.Hernandez@ars.usda.gov

Citation:

Hernandez, M., Nearing, M. A., Al-Hamdan, O. Z., Pierson, F. B., Armendariz, G., Weltz, M. A., . . . Holifield Collins, C. D. (2017). The rangeland hydrology and erosion model: A dynamic approach for predicting soil loss on rangelands. *Water Resources Research*, 53, 9368–9391. <https://doi.org/10.1002/2017WR020651>






Received 24 FEB 2017

Accepted 6 SEP 2017

Accepted article online 12 SEP 2017

Published online 18 NOV 2017

The Rangeland Hydrology and Erosion Model: A Dynamic Approach for Predicting Soil Loss on Rangelands

Mariano Hernandez¹ , Mark A. Nearing¹, Osama Z. Al-Hamdan², Frederick B. Pierson³, Gerardo Armendariz¹, Mark A. Weltz⁴, Kenneth E. Spaeth⁵, C. Jason Williams¹ , Sayjro K. Nouwakpo⁶ , David C. Goodrich¹ , Carl L. Unkrich¹, Mary H. Nichols¹ , and Chandra D. Holifield Collins¹

¹U.S. Department of Agriculture, Agricultural Research Service, Southwest Watershed Research Center, Tucson, AZ, USA,

²Department of Civil and Architectural Engineering, Texas A&M University-Kingsville, Kingsville, TX, USA, ³U.S. Department of Agriculture, Agricultural Research Service, Northwest Watershed Research Center, Boise, ID, USA, ⁴U.S. Department of Agriculture, Agricultural Research Service, Great Basin Rangelands Research, Reno, NV, USA, ⁵U.S. Department of Agriculture, Natural Resources Conservation Service, Central National Technology Support Center, Ft. Worth, TX, USA,

⁶Department of Natural Resources and Environmental Science, University of Nevada Reno, Reno, NV, USA

Abstract In this study, we present the improved Rangeland Hydrology and Erosion Model (RHEM V2.3), a process-based erosion prediction tool specific for rangeland application. The article provides the mathematical formulation of the model and parameter estimation equations. Model performance is assessed against data collected from 23 runoff and sediment events in a shrub-dominated semiarid watershed in Arizona, USA. To evaluate the model, two sets of primary model parameters were determined using the RHEM V2.3 and RHEM V1.0 parameter estimation equations. Testing of the parameters indicated that RHEM V2.3 parameter estimation equations provided a 76% improvement over RHEM V1.0 parameter estimation equations. Second, the RHEM V2.3 model was calibrated to measurements from the watershed. The parameters estimated by the new equations were within the lowest and highest values of the calibrated parameter set. These results suggest that the new parameter estimation equations can be applied for this environment to predict sediment yield at the hillslope scale. Furthermore, we also applied the RHEM V2.3 to demonstrate the response of the model as a function of foliar cover and ground cover for 124 data points across Arizona and New Mexico. The dependence of average sediment yield on surface ground cover was moderately stronger than that on foliar cover. These results demonstrate that RHEM V2.3 predicts runoff volume, peak runoff, and sediment yield with sufficient accuracy for broad application to assess and manage rangeland systems.

1. Introduction

The complex interactions of climate change, vegetation, surface soil dynamics, and human activities have major impacts on runoff and soil erosion processes on rangeland ecosystems. These processes and activities affect ecosystem function over a wide range of spatial and temporal scales (Williams et al., 2016b). Nearing et al. (2004) suggested that climatic variability will increase erosion in the future in many environments. That is, extreme climate events are expected to lead to a more vigorous hydrological cycle, including total rainfall amount and variability, and more frequent high-intensity rainfall events that drive water erosion processes (Nearing et al., 2004, 2015). Rangeland degradation such as declining vegetation cover, shifts in vegetation composition, and associated losses in ecosystem productivity are likely consequences of cyclic climate events (United Nations Convention to Combat Desertification (UNCCD), 1994). Decades of research have shown that rangelands can sustainably produce a variety of goods and services even in the face of extreme climatic events if managers respond quickly and appropriately to changes (Havstad et al., 2009). While land managers may not be able to reduce the progress of climate change through mitigation, they may be able to adapt to climate change and devise management practices that are more resilient and resistant to climate impacts. Soil erosion is among the climate-related impacts that concern rangeland managers since conservation of topsoil is critical to sustained productivity in rangeland ecosystems. Soil loss rates on rangelands are regarded as one of the few quantitative indicators for assessing rangeland health and conservation practice effectiveness (Nearing et al., 2011; Weltz et al., 2014a).

Future erosion prediction technology must be capable of simulating the complex interactions among vegetation characteristics, surface soil properties and hydrologic and erosion processes on rangelands according to Nearing and Hairsine (2011). Furthermore, Al-Hamdan et al. (2012b) pointed out that better representation of the temporal dynamics of soil erodibility related to disturbed rangeland conditions (e.g., fire) is also needed.

In rangelands, it is the rare precipitation event (e.g., return period greater than 10 years) which may trigger a nick-point along the hillslope that can degrade the site's stability and hydrologic function by allowing water to concentrate and accelerate soil loss (Nearing et al., 1997; Weltz et al., 2014b). As rangelands are not tilled, these flow channels and rills persist and can act to rapidly convey raindrop splash detached sediments down the hillslope in future runoff events (Davenport et al., 1998; Wilcox et al., 1996). Protected vegetated surfaces between flow channels and rills are safe sites, resulting in minor runoff and low sediment yield from these areas (Davenport et al., 1998; Okin et al., 2015; Puigdefabregas, 2005; Ravi et al., 2010; Urgeghe & Bautista, 2015; Wilcox et al., 2003). The same landscape with uniform soil disturbance and distribution of vegetation may experience significantly more runoff and soil loss from a similar runoff event due to increased connectivity of bare soils and formation of well-organized concentrated flow paths (Williams et al., 2016a).

Several studies have documented increases in peak flows and erosion occurring on systems that have been altered by some disturbance. Spaeth (1990) found that vegetation related variables such as foliar cover and biomass are more correlated with runoff and erosion rates during the initial phase of a rainfall event. As the storm progresses in time, soil related variables are more highly correlated with hydrology and erosion rates. Pierson et al. (2002) and Pierson and Williams (2016) found that burning may increase runoff, erosion, or both during high-intensity rainfall events by factors of 2–40 over small-plots scales and more than 100-fold over large-plot to hillslope scales. Results from rainfall simulator experiments suggest that erosion rates are much higher in the early part of a runoff event than in the latter part of the event on forest roads (Foltz et al., 2008) and burned rangeland (Pierson et al., 2008, 2011). These rapid changes in the concentrated flow erosion rate on disturbed soils may be caused by the winnowing of fine or easily detached soil particles during the early stages of erosive runoff, thus leaving larger or more embedded particles and/or soil aggregates which require greater stream power for detachment (Robichaud et al., 2010).

It is these high runoff events and corresponding high soil losses that have the greatest impact on long-term sustainability of rangelands. The ability to predict erosion from such events is required if land managers are going to make informed decisions on how to alter current practices to enhance sustainability of rangelands. RHEM has the ability to apply such analysis to both undisturbed soils and disturbed soils.

In 2006, the USDA-Agricultural Research Service (USDA-ARS) developed the Rangeland Hydrology and Erosion Model (RHEM) V1.0, which used physical-based concepts from the state-of-the-art technology from the Water Erosion Prediction Project (WEPP) (Flanagan & Nearing, 1995). However, the basic equations in the WEPP model are based on experimental data from croplands. While many of the fundamental hydrologic and erosion processes can be expressed in a common way on both croplands and rangelands, there were several aspects of the WEPP model that are not optimal for rangeland application and hence were modified, dropped, or replaced in RHEM (Nearing et al., 2011). On rangelands, vegetation can consist of varying composition of trees, shrubs, graminoids, forbs, and undisturbed soils from cultivation.

RHEM V1.0 was initially developed for undisturbed rangelands where the impact of concentrated flow erosion is limited and most soil loss occurs by rain splash and sheet erosion processes. RHEM V1.0 included a new splash and sheet equation developed by Wei et al. (2009) based on rainfall simulation data collected on rangeland plots from the WEPP and Interagency Rangeland Water Erosion Team (IRWET) (Interagency Rangeland Water Erosion Team and National Rangeland Study Team (IRWET & NRST), 1998) projects, which together covered 49 rangeland sites distributed across 15 western states. WEPP uses two methods of computing the peak discharge; a semianalytical solution of the kinematic wave model (Stone et al., 1995) and an approximation of the kinematic wave model that was developed to reduce run times on computers of two decades ago. The first method is used when WEPP is run in a single event mode while the second is used when WEPP is run in a continuous simulation mode. In RHEM V1.0, the semianalytical solution of the kinematic wave model was used instead of the approximate method for calculating peak runoff. Furthermore, RHEM V1.0 adapted WEPP's steady state cropland-based shear stress approach for modeling

concentrated flow erosion. Consequently, it was not possible to quantify within-storm sediment dynamics (Bulygina et al., 2007). That is, a steady state model does not allow the user to represent changing parameter values, such as soil erodibility, during the rainfall event. It also does not provide information on peak sediment discharge or the sediment load pattern within the storm, both of which can be useful for designing appropriate management alternatives that reduce sediment losses (Kalin et al., 2004). RHEM V1.0 uses the Yalin sediment transport capacity equation (Yalin, 1963) and the shear stress partitioning detachment and deposition concepts developed by Foster (1982), which distributes the transport capacity among various particle types. RHEM 1.X provided reasonable erosion rates based on findings from rainfall simulation studies on undisturbed rangeland soils (Nearing et al., 2011).

Versions of RHEM V2.0 and greater are fundamentally a different model than previous versions because of changes to critical hydrologic and soil erosion prediction equations (Al-Hamdan et al., 2015). They include the integration of the dynamic formulation of a stream power sediment continuity equation (Bennett, 1974) instead of the steady state shear stress approach for modeling concentrated flow erosion. Nearing et al. (1997) and others found that the best predictor for unit sediment load was stream power instead of shear stress, unit stream power, and effective stream power. Stream power produced a higher level of statistical fit to the sediment load. Furthermore, Al-Hamdan et al. (2012b) used concentrated flow simulations on disturbed and undisturbed rangeland to estimate soil erodibility as well as to evaluate the performance of linear and power law equations that describe the relationship between erosion rate and several hydraulic parameters. They showed that stream power provided the best linear function to describe the detachment rate on disturbed rangeland sites. Based on these findings, we integrated the empirical equation developed by Nearing et al. (1997) to calculate the sediment transport capacity into RHEM V2.0. In subsequent versions of RHEM leading to V2.3, major changes have been implemented to the parameter estimation equations for describing and quantifying disturbed rangelands and testing the model efficiency in predicting larger soil loss events. The main structure of the RHEM V2.3 model has not changed significantly from previous versions (Al-Hamdan et al., 2015).

The enhanced RHEM V2.3 model provides major advantages over existing erosion model prediction technology, including RHEM V1.0. RHEM V2.3 is capable of capturing the influence of different plant growth/life forms, disturbances such as fire, climate change, and rangeland management practices on important hydrological and erosion processes acting on rangelands. RHEM has undergone critical review and expansion of capabilities. The most significant differences between this model and the original are: (1) the model uses a dynamic solution of the sediment continuity equation based on kinematic wave routing of runoff, and the integration of the newly developed splash and sheet source term equation, and stream power for predicting sediment transport of concentrated flow erosion (Nearing et al., 1997); (2) it integrates the approach for estimating the splash and sheet erodibility coefficients formulated by Al-Hamdan et al. (2017), who developed equations to predict the differences of erodibility before and after disturbance across a wide range of soil texture classes and vegetation cover types; (3) the model integrates the method for predicting concentrated flow erosion based on the work by Al-Hamdan et al. (2012b), who developed a dynamic erodibility approach for modeling concentrated flow erosion (e.g., for sites with relatively immediate disturbance, such as fire); and (4) the model includes a user-friendly web-based interface to allow users to simplify the use of RHEM, manage scenarios, centralize scenario results, compare scenario results, and provide tabular and graphical results (Hernandez et al., 2015).

RHEM has been applied successfully to illustrate the influence of plant and soil characteristics on soil erosion and hydrologic function in Major Land Resource Area 41 (MLRA 41-Southeastern Basin and Range) located in the southern U.S. (Hernandez et al., 2013). Moreover, RHEM has been employed to assess nonfederal rangeland soil loss rates at 10,000 National Resources Inventory (NRI) plot sites in the 17 States lying wholly or partly west of the 100th meridian for determining areas of vulnerability to accelerated soil loss using USDA Natural Resources Conservation Services (NRCS) NRI data (Spaeth et al., 2003, 2005; Weltz et al., 2014a). Williams et al. (2016b) used RHEM to predict runoff and erosion rates for refinement and development of Ecological Site Descriptions, and Hernandez et al. (2016) applied the model to characterize rangeland conditions based on a probabilistic approach subject to the presence of a set of soil erosion thresholds.

The goals of this paper are to describe the improved version of the RHEM V2.3 model by providing a detailed presentation of the mathematical model structure and to report the results of model applications.

We also demonstrate gains in model performance and reliability over the former model version RHEM V1.0. The objectives of this study are to: (1) present the foundational equations for the improved RHEM V2.3 model; (2) calibrate the RHEM V2.3 model using 23 rainfall-runoff-sediment yield events on a small semiarid subwatershed within the Walnut Gulch Experimental Watershed (WGEW) in Arizona, and compare them against parameters estimated by the RHEM V2.3 parameter estimation equations; (3) examine performance improvement from RHEM V1.0 to RHEM V2.3; and (4) present a case study application for evaluating the overall influence of foliar cover, surface ground cover, and annual rainfall on soil erosion rates from rangelands using 124 NRI plots in Arizona and New Mexico.

2. Material and Methods

This section is divided into four main parts as follows: (1) presentation of fundamental hydrologic and erosion equations in RHEM V2.3; (2) an overview of the RHEM V2.3 parameter estimation equations; (3) model calibration with the Model-Independent Parameter ESTimation (PEST) program; and, (4) statistical analysis and results.

2.1. Fundamental Hydrologic and Erosion Equations

2.1.1. Overland Flow Model

The hydrology component of the enhanced RHEM V2.3 model is based on the KINEROS2 model (Goodrich et al., 2012; Smith et al., 1995). The model was implemented to simulate one-dimensional overland flow within an equivalent overland flow modeling element representing a hillslope with uniform or curvilinear slope profiles. The flow per unit width across a plane surface as a result of rainfall can be described by the one-dimensional continuity equation (Woolhiser et al., 1990). Table 1 presents the fundamental overland flow equations driving the surface flow component in RHEM V2.3.

In equation (1), h is the flow depth at time t and the position x , x is the space coordinate along the direction of flow, and q is the volumetric water flux per unit plane width ($\text{m}^2 \text{s}^{-1}$). In equation (2), $\sigma(x, t)$ is the rainfall excess (m s^{-1}), where r is the rainfall rate (m s^{-1}), and f is the infiltration rate (m s^{-1}). Equation (3) represents the relationship between q and h , where g is the gravity acceleration (m s^{-2}), S is the slope gradient (m m^{-1}), and f_t is the total Darcy-Weisbach friction factor estimated using equation (18) in this paper developed by Al-Hamdan et al. (2013). Substituting equations (2) and (3) in equation (1) results in the hydrology routing equation (4) presented by Al-Hamdan et al. (2015). In RHEM, for a single hillslope element, the upstream boundary in equation (5) is assumed to be at zero depth and the downstream boundary is a continuing plane (along the direction of flow).

The infiltration rate is computed in KINEROS2 using equation (6), the three-parameter infiltration equation (Parlange et al., 1982), in which the models of Green and Ampt (1911) and Smith and Parlange (1978) are included as two limiting cases. Here l is the cumulative depth of the water infiltrated into the soil (m), K_e is the surface effective saturated hydraulic conductivity (m s^{-1}), C_d (m) accounts for the effect of capillary forces on moisture absorption during infiltration, and α is a scaling parameter. When $\alpha = 0$, equation (6) is reduced to the simple Green and Ampt infiltration model, and when $\alpha = 1$, the equation simplifies to the Parlange model. Most soils exhibit infiltrability behavior intermediate to these two models, and KINEROS2 uses a weighting α value of 0.85 (Smith et al., 1993). The state variable for infiltrability is the initial water content, in the form of the soil saturation deficit, $B = C_d(\theta_s - \theta_i)$, defined as the saturated moisture content minus the initial moisture content. The saturation deficit ($\theta_s - \theta_i$) is one parameter because θ_s is fixed from storm to storm. For ease of estimation, the KINEROS2 input parameter for soil water is a scaled moisture content, $S = \theta/\phi$, (ϕ is the soil porosity) which varies from 0 to 1. Initial soil conditions are represented by the variable S_i ($=\theta_i/\phi$). Thus, there are two parameters, K_e and C_d to characterize the soil, and the variable S_i to characterize the initial condition.

2.1.2. Overland Soil Erosion, Deposition, and Transport

Table 2 presents the surface erosion and sediment transport equations in RHEM V2.3. Equation (7) is the dynamic sediment continuity equation to describe the movement of suspended sediment in a concentrated flow area (Bennett, 1974), where C is the measured sediment concentration (kg m^{-3}), q_r is the flow discharge of concentrated flow per unit width ($\text{m}^2 \text{s}^{-1}$), D_{ss} is the splash and sheet detachment rate ($\text{kg s}^{-1} \text{m}^{-2}$), and

Table 1
Overland Flow Equations in RHEM V2.3

$\frac{\partial h}{\partial t} + \frac{\partial q}{\partial x} = \sigma(x, t)$	(1)
$\sigma(x, t) = r - f$	(2)
$q = \left(\frac{8gS}{f_t} \right)^{1/2} h^{3/2}$	(3)
$\frac{\partial h}{\partial t} + \frac{3}{2} \left(\frac{8gS}{f_t} \right)^{1/2} h^{1/2} \frac{\partial h}{\partial x} = r - f$	(4)
$h(0, t) = 0$	(5)
$f = K_e \left[1 + \frac{\alpha}{\exp\left(\frac{\alpha l}{C_d \Delta \theta_i}\right) - 1} \right]$	(6)

Table 2
Overland Soil Erosion, Deposition, and Transport Equations in RHEM V2.3

$$\begin{aligned} \frac{\partial(Ch)}{\partial t} + \frac{\partial(Cq_r)}{\partial x} &= D_{ss} + D_{cf} & (7) \\ q_r &= \frac{q}{w} & (8) \\ w &= \frac{2.46 Q^{0.39}}{S^{0.4}} & (9) \\ D_{ss} &= K_{ss} r^{1.052} \sigma^{0.592} & (10) \\ D_{cf} &= \begin{cases} D_c \left(1 - \frac{CQ}{T_c}\right), & CQ \leq T_c \\ \frac{0.5 V_f}{Q} (T_c - CQ), & CQ \geq T_c \end{cases} & (11) \\ D_c &= K_{\omega}(\omega) & (12) \\ \log_{10} \left(\frac{10T_c}{w} \right) &= -34.47 + 38.61 * \frac{\exp[0.845 + 0.412 \log(1000\omega)]}{1 + \exp[0.845 + 0.412 \log(1000\omega)]} & (13) \\ D_c &= K_{\omega(Max)adj} \exp(\beta q_c) \omega & (14) \\ q_c &= \int q_r dt & (15) \\ \omega &= \gamma S q_r & (16) \end{aligned}$$

D_{cf} is the concentrated flow detachment rate ($\text{kg s}^{-1} \text{m}^{-2}$). For a unit wide plane (overland flow element), when overland flow accumulates into a concentrated flow path, equation (8) calculates the concentrated flow discharge per unit width (q_r), where w in equation (8) is the concentrated flow width (m), equation (9) from Al-Hamdan et al. (2012a). The splash and sheet detachment rate (D_{ss}) is calculated using equation (10) developed by Wei et al. (2009), where K_{ss} is the splash and sheet erodibility, r (m s^{-1}) is the rainfall intensity, and σ is rainfall excess (m s^{-1}).

RHEM has the capability to estimate transport and erosion in ephemeral (rills) or semipermanent microchannels on the hillslopes of up to a few cm in width and depth. Concentrated flow detachment rate (D_{cf}) in equation (11) is calculated as the net detachment and deposition rate (Foster, 1982), where D_c is the concentrated flow detachment capacity ($\text{kg s}^{-1} \text{m}^{-2}$), Q is the flow discharge ($\text{m}^3 \text{s}^{-1}$), T_c is the sediment transport capacity (kg s^{-1}), and V_f is the soil particle fall velocity (m s^{-1}) that is calculated as a function of particle density and size (Fair & Geyer, 1954).

The sediment detachment rate from the concentrated flow is calculated by employing soil erodibility characteristics of the site and hydraulic parameters of the flow such as flow width and stream power. Soil detachment is assumed to start when concentrated flow starts (i.e., no threshold concept for initiating detachment is used) (Al-Hamdan et al., 2012b). To calculate D_c , equation (12) is used (Al-Hamdan et al., 2012b), where K_{ω} is the stream power erodibility factor ($\text{s}^2 \text{m}^{-2}$) and ω is the stream power (kg s^{-3}). We implemented the empirical equation developed by Nearing et al. (1997), equation (13), to calculate the transport capacity (T_c).

Soil detachment is not considered a selective process, so the sediment particles size distribution generated from actively eroding areas is assumed to be a function of the fraction of total sediment load represented by five particle classes based on soil texture.

RHEM V2.3 is a dynamic model and contains an option, to use equations (14)–(16) developed by Al-Hamdan et al. (2012b) for characterizing events on recently disturbed rangelands with high concentrated flow erodibility at the onset of the event and with exponentially decreasing erodibility throughout the event due to reduction in sediment availability (winnowing of readily available sediment). $K_{\omega(Max)adj}$ is the maximum stream power erodibility ($\text{s}^2 \text{m}^{-2}$) corresponding to the decay factor β [$\beta = -5.53 (\text{m}^{-2})$], a decay coefficient representing erodibility change during an event, ω is the stream power (kg s^{-3}), q_c is the cumulative flow discharge of concentrated flow per unit width (m^2), γ is the water specific weight ($\text{kg m}^{-2} \text{s}^{-2}$), and S is the slope gradient (m m^{-1}).

2.1.3. Model Limitations

KINEROS2 has a number of limitations: (1) It is event-based and it does not treat snowmelt, lateral subsurface flow, or biogeochemistry (Goodrich et al., 2012), and (2) It simulates runoff and erosion only for small watersheds (Schaffner et al., 2010). As such KINEROS2 does not address flow in channels. The transport capacity equation of Nearing et al. (1997) does not account for particle sorting. Consequently, routing of sediment by size particle is not carried out. RHEM is a hillslope scale model.

KINEROS2 has been coupled with Opus2 (Müller et al., 2003) to form a continuous model (K2-O2: <https://www.tucson.ars.ag.gov/k2o2/doku.php>) that treats intra-storm runoff and erosion processes and interstorm biogeochemistry, plant growth, and soil moisture redistribution.

2.2. RHEM Model Parameter Estimation Equations

An important aspect of RHEM with regards to application by rangeland managers is that plant life/growth forms and surface ground cover using data commonly collected in rangeland inventory and assessment efforts (e.g., rangeland health or NRI assessments) are used in parameterization of RHEM. Plant life/growth forms are characterized as bunchgrasses, sodgrasses, shrubs, and forbs/annual grasses. Ground cover is characterized as rock, litter, basal cover, and biological soil crusts. Biological soil crusts are an association

between soil particles and nonvascular plants (cyanobacteria, algae, microfungi, lichens, and bryophytes) which live on top or within the upper few millimeters of the soil surface (Belnap, 2006; Rosentreter et al., 2007). Historically these communities have been known by a variety of names, including cryptobiotic, cryptogamic, and microbiotic soil crusts but now are commonly called biological soil crusts. They are found in all dryland regions of the world and in all vegetation types. In RHEM, the acronym used with predictive equations uses the older name of *cryptogams* or *crypto*. We retained these acronyms to be consistent with the original publications for readers interested in tracking the science backwards through these publications.

2.2.1. Effective Saturated Hydraulic Conductivity

Research has indicated that infiltration, runoff, and erosion dynamics are correlated with the presence/absence and composition of specific plant taxa and growth attributes (Davenport et al., 1998; Ludwig et al., 2005; Pierson et al., 2010, 2013; Spaeth et al., 1996; Turnbull et al., 2012; Wainwright et al., 2000; Wilcox et al., 2012; Williams et al., 2014b). Numerous studies have documented that infiltration of rainfall increases with increasing vegetative surface cover (Ludwig et al., 2005). For example, Tromble et al. (1974) evaluated infiltrability on three range sites in Arizona and found infiltrability was positively related to vegetal cover and litter biomass and negatively related to gravel cover. Meeuwig (1970) and Dortignac and Love (1961) also found infiltrability and litter cover to be positively related. Work by Spaeth et al. (1996) using data from across the western U.S. concluded that inclusion of specific plant species and ground cover variables in prediction equations significantly improved infiltration estimation as opposed to using functional cover groups such as total canopy and foliar cover. Thompson et al. (2010) provide a detailed review of research findings on vegetation-infiltration relationships across climate and soil type gradients.

Soil texture may be used as the first estimator of K_e because texture affects the pore space available for water movement. Also, soil texture is easy to measure and often available for an area of interest. Rawls et al. (1982) developed a look-up table of saturated hydraulic conductivity, K_s , values for the 11 USDA soil textural classes. Bulk density is another basic soil property that is related to pore space and water movement. Rawls et al. (1998) revised the texture-based look-up table to include two porosity classes and two bulk density classes within each textural class, the geometric means of the K_s along with the 25% and 75% percentile values. The texture/porosity K_s estimates were based on a national database of measured K_s values and soil properties at 953 locations. These estimates indicate that (1) K_s is highest for coarse-textured soils and (2) within a textural class, soils with greater porosity (lower bulk density) have higher K_s values (Rawls et al., 1998).

Saturated hydraulic conductivity has been characterized as being lognormally distributed in space (Smith & Goodrich, 2000), with variations of an order of magnitude or more across relatively short distances. It is clear that representing a landscape using various values of saturated conductivity distributed across space with a lognormal distribution is more realistic than a single uniformly applied mean value. Stone et al. (1992) developed an exponential model to adjust the baseline saturated hydraulic conductivity (Rawls et al., 1982) as a function of surface cover and foliar cover based on an unpublished analysis of rainfall simulator data on desert brush dominated sites in Arizona and Nevada. Moreover, they divided the baseline saturated hydraulic conductivity by two to account for the effects of crusting on the effective saturated hydraulic conductivity. However, Stone et al. (1992) did not report criteria to assess the goodness of fit of the model and the range of values of the predictor variables. In the model developed by Stone et al. (1992), the effective saturated hydraulic conductivity increases exponentially as ground cover and foliar cover increases, which is consistent with the trend shown in croplands reported by Rawls et al. (1990) and Zhang et al. (1995). Moreover, as pointed out by Zhang et al. (1995), for accurate simulation of the effects of foliar cover on infiltration and runoff, the impact of canopy height must be considered.

In this study, baseline hydraulic conductivity values were defined based on the 25% and 75% percentile values for each soil textural class reported by Rawls et al. (1998). Then we adjusted them to account for the effects of litter and basal cover based on Stone et al. (1992) as follows:

$$K_{e_i} = K_{b_i} e^{[p_i(litter + basal)]} \quad (17)$$

In this equation, K_{b_i} is the 25% percentile saturated hydraulic conductivity for each soil textural class, i , reported by Rawls et al. (1998). p is defined as the natural log of the ratio of the 75% to the 25% percentile values of saturated hydraulic conductivity; *litter* is litter cover (expressed as a fraction); and *basal* is basal

area cover (expressed as a fraction). The analysis carried out by Nearing et al. (2011) on rainfall simulator data showed that for similar levels of plant cover and soils, K_{ei} was approximately 20% less for the sodgrasses compared to the bunchgrasses, forbs, and annuals, while K_{ei} was approximately 20% greater for the shrubs. Hence, we adjusted the K_{ei} value computed by equation (17) by 1.2 and 0.8, respectively, when using the model for shrub and sodgrass communities.

2.2.2. Hydraulic Roughness Coefficient

Al-Hamdan et al. (2013) developed empirical equations that predict the total measured friction factor (f_t) by regressing the total measured friction against the measured vegetation and rock cover, slope, and flow rate. All equations derived by Al-Hamdan et al. (2013) showed that basal plant cover exerted the most influence, and had the most important effect on total friction among other measured cover attributes.

RHEM computes the total Darcy-Weisbach friction (f_t) factor estimated by Al-Hamdan et al. (2013) as follows:

$$\log(f_t) = -0.109 + 1.425 \text{ litter} + 0.442 \text{ rock} + 1.764 (\text{basal} + \text{cryptogams}) + 2.068 S \quad (18)$$

where *litter* is the fraction of area covered by litter to total area ($\text{m}^2 \text{m}^{-2}$), *basal* and *cryptogams* is the fraction of area covered by basal plants and biological soil crust cover to total area ($\text{m}^2 \text{m}^{-2}$), *rock* is the fraction of area covered by rock to total area ($\text{m}^2 \text{m}^{-2}$), and *S* is the slope gradient (m m^{-1}).

2.2.3. Splash and Sheet Erodibility Factor

The RHEM model parameterization represents erosion processes on undisturbed rangelands, as well as rangelands that show disturbances such as fire or woody plant encroachment (Al-Hamdan et al., 2017; Hernandez et al., 2013; Nearing et al., 2011; Williams et al., 2016b). In RHEM, soil detachment is predicted as a combination of two erosion processes, rain splash and thin sheet flow (splash and sheet) detachment and concentrated flow detachment.

This section presents empirical equations developed by Al-Hamdan et al. (2017) using piecewise regression analysis to predict splash and sheet erodibility across a broad range of soil texture classes based on vegetation cover and surface slope gradient.

Bunch Grass:

$$\text{Log}_{10} K_{ss} = \begin{cases} 4.154 - 2.547 * G - 0.7822 * F + 2.5535 * S & \text{if } G \leq 0.475 \\ 3.1726975 - 0.4811 * G - 0.7822 * F + 2.5535 * S & \text{if } G > 0.475 \end{cases} \quad (19)$$

Sod Grass:

$$\text{Log}_{10} K_{ss} = \begin{cases} 4.2169 - 2.547 * G - 0.7822 * F + 2.5535 * S & \text{if } G \leq 0.475 \\ 3.2355975 - 0.4811 * G - 0.7822 * F + 2.5535 * S & \text{if } G > 0.475 \end{cases} \quad (20)$$

Shrub:

$$\text{Log}_{10} K_{ss} = \begin{cases} 4.2587 - 2.547 * G - 0.7822 * F + 2.5535 * S & \text{if } G \leq 0.475 \\ 3.2773975 - 0.4811 * G - 0.7822 * F + 2.5535 * S & \text{if } G > 0.475 \end{cases} \quad (21)$$

Forbs:

$$\text{Log}_{10} K_{ss} = \begin{cases} 4.1106 - 2.547 * G - 0.7822 * F + 2.5535 * S & \text{if } G \leq 0.475 \\ 3.1292975 - 0.4811 * G - 0.7822 * F + 2.5535 * S & \text{if } G > 0.475 \end{cases} \quad (22)$$

where *G* is the area fraction of ground cover, *F* is the area fraction of foliar cover, and *S* is the slope gradient (expressed as a fraction).

Al-Hamdan et al. (2017) reported that RHEM performed well using K_{ss} and setting the concentrated flow erodibility coefficient (K_w) to the default value of $7.747 \times 10^{-6} (\text{s}^2 \text{m}^{-2})$ in RHEM V2.2. According to Al-Hamdan et al. (2017), this is a small value of concentrated flow erodibility typical for undisturbed rangeland. Furthermore, they assumed that the sediment detachment was dominated by raindrop impact and thin sheet flow as long as the small concentrated flow paths on the rainfall simulator plots work primarily as the transport mechanism for the splash and sheet-generated sediments. The K_{ss} equation that represents the dominant vegetation community in the site to be evaluated should be used. However, if the site does not

have a dominant vegetation form or more details are needed, then weight averaging between equations (19) and (22) based on the percentage of life form can be used. K_{ss} is multiplied by 1.3 to account for the bias in predictions from the exponential relationships (Duan, 1983).

2.2.4. Concentrated Flow Erodibility Coefficients for Hillslope Microchannels

The model has integrated an equation developed by Al-Hamdan et al. (2012b) to calculate K_{ω} for a broad range of undisturbed rangeland sites in which rills are active, but sediment availability is low (e.g., extensive bare ground, but limited loose sediments, long eroded sites, etc.).

$$\log_{10}(K_{\omega}) = -4.14 - 1.28 \text{ litter} - 0.98 \text{ rock} - 15.16 \text{ clay} + 7.09 \text{ silt} \quad (23)$$

The model also has the capacity, as an option, to use equations developed by Al-Hamdan et al. (2012b) for predicting maximum erodibility needed in equation (14) for a wide range of burned rangeland sites including burned tree encroached sites. This parameterization of $K_{\omega(\max)adj}$ is needed in the special case of abrupt disturbance (e.g., post-fire, instantly available sediment pulse) where rills are actively eroding and soil is not limited, with steep slope gradients (>20%), and exposed loose soil (Al-Hamdan et al., 2017).

$$\log_{10}(K_{\omega(\max)adj}) = -3.64 - 1.97(\text{litter} + \text{basal} + \text{crypto}) - 1.85 \text{ rock} - 4.99 \text{ clay} + 6.0 \text{ silt} \quad (24)$$

where *litter*, *basal*, and *crypto* are the fraction of area covered by litter, basal, and biological soil crust to total area ($\text{m}^2 \text{ m}^{-2}$), *rock* is the fraction of area covered by rock to the total area ($\text{m}^2 \text{ m}^{-2}$), and *clay* and *silt* are the respective surface soil fractions.

Using data from rainfall simulator experiments conducted on rangelands with a wide span of characteristics, Al-Hamdan et al. (2013) showed that formation of continuous concentrated flow paths at the plot scale is positively correlated with flow discharge per unit width, slope, and ground cover. Using the same data set, they developed a logistic equation to estimate the probability of overland flow to become concentrated on rangeland:

$$P = \frac{\exp(-6.397 + 8.335S + 3.252bare + 3440q)}{1 + \exp(-6.397 + 8.335S + 3.252bare + 3440q)} \quad (25)$$

where S is slope (m m^{-1}), *bare* is fraction of bare soil to total area ($\text{m}^2 \text{ m}^{-2}$), and q is flow discharge per unit width ($\text{m}^2 \text{ s}^{-1}$). Concentrated flow paths in RHEM are spaced in 1 m increments perpendicular to the hill-slope angle. This means that concentrated flow paths are always formed, and the distance between each flow path is 1 m. Therefore, the interpretation of P becomes the probability that overland flow will be a significantly highly erosive concentrated flow (Al-Hamdan et al., 2017).

2.3. PEST Model Parameterization

This study employs PEST software (Doherty, 2015) to calibrate RHEM parameters and evaluate model performance for the 23 rainfall-runoff-erosion events at the Lucky Hills 106 (LH106) subwatershed in the WGEW, southwestern Arizona, USA. The parameter calibration process included two approaches: first, the overland flow related parameters were calibrated (effective saturated hydraulic conductivity, total friction factor, and capillary drive); second, the calibration of the splash-and-sheet soil erodibility coefficient was achieved by keeping constant the optimized overland flow parameters and the concentrated flow erosion coefficient. It is assumed that contribution of channel sediment is negligible at LH106 (Nearing et al., 2007; Nichols et al., 2012). The parameters slope gradient and coefficient of variation for K_e were held constant during the calibration. A detailed description of the overland flow parameters can be found in Smith et al. (1995).

2.4. Statistical Analysis

Nash-Sutcliffe Efficiency (NSE) (Nash & Sutcliffe, 1970) between observed and calculated cumulative flows was calculated for each single event at LH106 as follows:

$$NSE = 1 - \frac{\sum_{t=1}^T (O_t - M_t)^2}{\sum_{t=1}^T (O_t - \bar{O})^2} \quad (26)$$

where O_t , \bar{O} , and M_t are observed cumulative flows at time step t , average cumulative value, and modeled cumulative flows at time step t , respectively. T is the total number of time steps in the simulation for each rainfall event.

Moreover, percent bias (PBIAS) (Gupta et al., 1999) and the RMSE-observations standard deviation ratio (RSR) (Moriiasi et al., 2007) were calculated to evaluate the overall performance of the model for runoff volume, peak runoff, and sediment yield estimates from the 23 events at LH106.

PBIAS was calculated by

$$PBIAS = \frac{\sum_{i=1}^N (O_i - M_i) * 100}{\sum_{i=1}^N O_i} \quad (27)$$

RSR was calculated by

$$RSR = \frac{\sqrt{\sum_{i=1}^N (O_i - M_i)^2}}{\sqrt{\sum_{i=1}^N (O_i - \bar{O})^2}} \quad (28)$$

where O_i is the observed value of event i , M_i is the model generated value for the corresponding event i , \bar{O} is the average of the observed values, and N is the total number of events at LH106.

3. Study Area and NRI Database

3.1. Lucky Hills 106 Watershed

Data used for the calibration and evaluation of the model were obtained from the USDA-ARS Southwest Watershed Research Center's Lucky Hills experimental site, located in the WGEW. The semiarid WGEW is located in southeastern Arizona (31°44.6'N, 110°3.2'W) and surrounds the town of Tombstone, Arizona (Figure 1). It has a mean annual temperature of 17.7°C and a mean annual precipitation of 350 mm, the majority

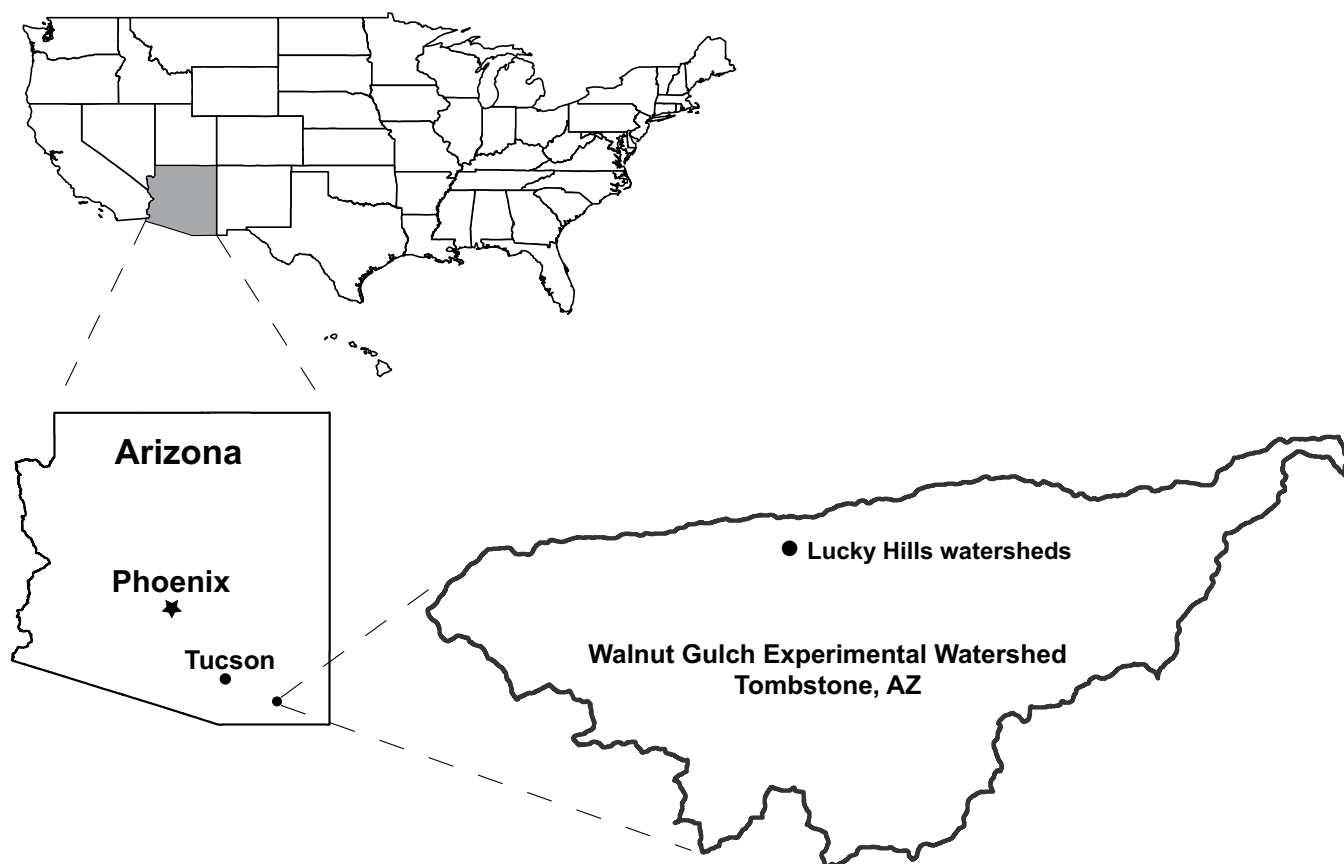


Figure 1. Location of the Lucky Hills subwatershed study area within the Walnut Gulch Experimental Watershed.

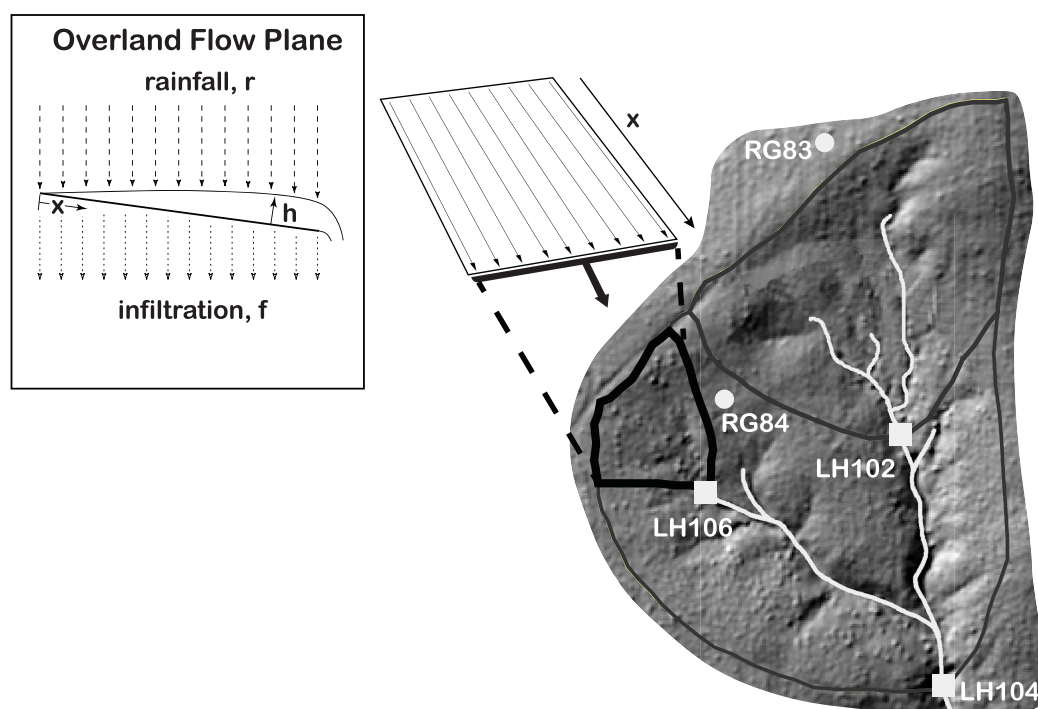


Figure 2. Lucky Hills 106 and its representation as an overland flow plane in the RHEM model.

of which is a result of high-intensity convective thunderstorms in the summer monsoon season (Keefer et al., 2015).

The LH106 subwatershed presents an excellent location for this study because of the availability of vegetation data and rainfall, runoff, sediment discharge, and soil moisture time series data. LH106 is extensively instrumented for hydrologic research and is subject to ongoing ecohydrologic studies by the USDA-ARS Southwest Watershed Research Center (Renard et al., 2008). LH106 also is appropriate because it is not channelized and acts more as a large hillslope rather than a watershed with significant contribution of channel sediment (Nearing et al., 2007; Nichols et al., 2012). The area and slope length for the subwatershed are 0.367 ha and 65.3 m, respectively. At this scale, rainfall amount and intensity, vegetative foliar cover, surface ground cover, and microtopography (and their spatial variability) largely determine overland flow, splash and sheet, and concentrated flow soil erosion processes (Lane et al., 1997).

Rainfall at the site is measured by a digital weighing-recording rain gage (Goodrich et al., 2008) and runoff and sediment discharge are measured by multiple weirs and an H-flume (Nearing et al., 2007). Rainfall and runoff data have been collected at Lucky Hills since 1963, when rain gauge 83 and weirs LH 104 and 102 were installed (Figure 2). Rainfall is recorded with a temporal resolution of 1 min (Figure 2). Rain gauge 84 was added in 1964 and an H-flume was installed on LH106 in 1965 (Figure 2) to collect suspended sediment samples in addition to the coarse load deposited in the flume during each event (Simanton et al., 1993). Since the instrumentation was installed in the early 1960s, rainfall and runoff data have been collected with only short interruptions for upgrading equipment, which occurred during the winter (Renard, 1980). Soil moisture is measured at multiple depths at each rain gage using Time Domain Reflectometry (TDR) sensors (Keefer et al., 2008).

The vegetation at LH106 is comprised mostly of shrubs on an 8% slope gradient. Dominant shrubs include creosote bush [*Larrea tridentata* (Sessé & Moc. ex DC.) Coville] and whitethorn acacia [*Acacia constricta* Benth.]. The shrubs are about 0.6 m high and cover about 25% of the surface during the rainy seasons. Approximately two-thirds of the ground area is covered with rock and the remaining one-third is bare soil (Nearing et al., 2007). A sparse understory of grasses and forbs is also found (Weltz et al., 1994). Foliar and ground cover information is given in Table 3. The soil is a Lucky Hills-McNeal gravelly sandy loam complex with approximately 52% sand, 26% silt, and 10% clay on a Limy Uplands (12–16" p.z.) ecological site. Average rock fragment by volume for LH106 was reported as 30% (Woolhiser et al., 1990), which is in agreement

Table 3
Summary of the Surface Ground Cover and Foliar Cover for Lucky Hills 106 Subwatershed

Cover			
Ground Surface	(%)	Foliar	(%)
Basal	5	Bunch Grass	0
Rock	45	Forbs/Annual Grasses	0
Litter	5	Shrub	25
Biological soil crust	0	Sod Grass	0
Total	55	Total	25

with the rock fragment content by volume for gravelly sandy loam reported by Schoeneberger et al. (2012). A 1 m \times 1 m DEM was prepared from LIDAR survey and used to define the microtopography characteristics.

We used 23 time-intensity pairs collected between 2005 and 2010 from rain gauge 83 as an input into the RHEM model to assess the hydrologic and erosion response of LH106 (Figure 2). Summary descriptive statistics of volumetric soil moisture, rainfall, observed runoff volume, observed peak runoff, and observed sediment yield are presented in Table 4.

3.2. National Resources Inventory Field Measurements and Data Description

A major data source for rangeland assessment on nonfederal lands is the National Resources Inventory (Nusser & Goebel, 1997; Spaeth et al., 2003). A review of new proposed NRI protocols on nonfederal rangelands is presented in the National Resources Inventory Handbook of Instructions for Rangeland Field Study Data Collection (United States Department of Agriculture (USDA), 2014), and a summary of NRI results on rangeland is presented in Herrick et al. (2010). The USDA-NRCS provided data for 542 NRI points collected between 2003 and 2014 across Arizona and New Mexico to parameterize the RHEM model. The points were grouped by soil texture classes, as follows: sand, sandy loam, silt loam, and clay loam. For this study, we selected only the sandy loam soil texture class to be in agreement with the LH106 soil texture class. We found 124 NRI points in the sandy loam group. The 124 NRI data points were further grouped into annual rainfall regimes measured at five weather stations. The Jornada weather station is located in New Mexico, and the Ganado, Laveen, Snowflake, and Willcox stations are in Arizona.

Next, surface ground cover, foliar cover, basal area, biological soil crust cover, litter cover, rock fragment cover, and slope gradient percent were estimated for the 124 NRI points. Figures 3–5 present the distributions for surface ground cover, foliar cover, and slope gradient grouped by annual rainfall amounts. For purposes of RHEM application, ground cover is the cover of the soil surface that essentially is in contact with the soil, as opposed to foliar cover, which is cover above the ground surface and provided by plants. Ground cover may be present in the form of plant litter, rock fragments, biological soil crusts, and plant bases/stems.

4. Results and Discussion

This section presents the simulation results corresponding to three sets of parameter values. The first set was obtained through the RHEM V2.3 parameter estimation equations presented in this paper. The second set was obtained through the model calibration using 23 rainfall-runoff events on the Lucky Hills 106 subwatershed. The third set was obtained through the RHEM V1.0 parameter estimation equations (Nearing et al., 2011). A comparison between simulation runs using RHEM V2.3 and RHEM V1.0 parameter estimation equations was carried out to evaluate the improvement in relation to the estimation of sediment yield in the Lucky Hills 106 subwatershed. At the end of this section, a case study of application of the RHEM V2.3 model on a number of sites using NRI points is presented.

4.1. Model Performance With RHEM V2.3 Parameter Estimation Equations

Total friction factor (f_t), equation (18), effective saturated hydraulic conductivity (K_e), equation (17), splash and sheet erodibility coefficient (K_{ss}), equations (19)–(22), and concentrated flow erodibility coefficient (K_{co}), equation (23), were determined for LH106 (Table 5).

The model performance based on the *PBIAS* and *RSR* goodness of fit criteria for runoff volume, peak runoff, and sediment yield at LH106 is shown in Table 6.

On the basis of the model performance criteria reported by Moriasi et al. (2007), model performance based on the *RSR* criterion can be

Table 4
Summary Descriptive Statistics of the 23 Events at Lucky Hills 106 and Rain Gauge 83

	Mean	Min	Max	Std
Volumetric soil moisture (%)	0.13	0.05	0.19	0.04
Rainfall Volume (mm)	21.86	8.64	46.35	12.08
Runoff Volume (mm)	7.63	2.10	22.82	6.06
Peak Runoff Rate (mm h ⁻¹)	38.34	11.92	106.56	24.01
Sediment Yield (t ha ⁻¹)	0.23	0.03	0.94	0.23

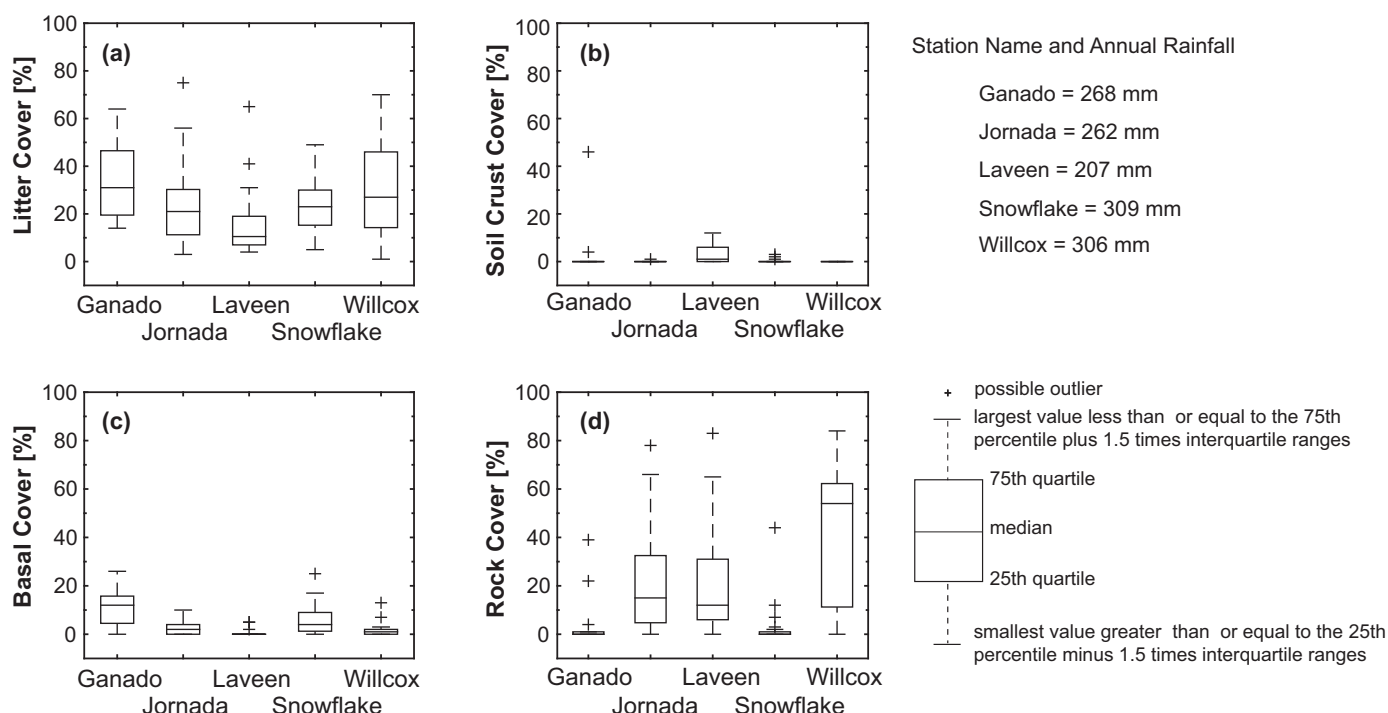


Figure 3. Distributions of surface ground cover grouped by the five weather stations. (a) Litter cover, (b) biological soil crust cover, (c) basal area, and (d) rock cover for the NRI points.

evaluated as “very good” if $0 \leq RSR \leq 0.50$, “good” if $0.50 < RSR \leq 0.60$, “satisfactory” if $0.60 < RSR \leq 0.70$; and “unsatisfactory” if $RSR > 0.70$. Therefore, these rankings suggest that RHEM performance can be evaluated as “satisfactory” for runoff volume, “good” for peak runoff and “very good” for sediment yield.

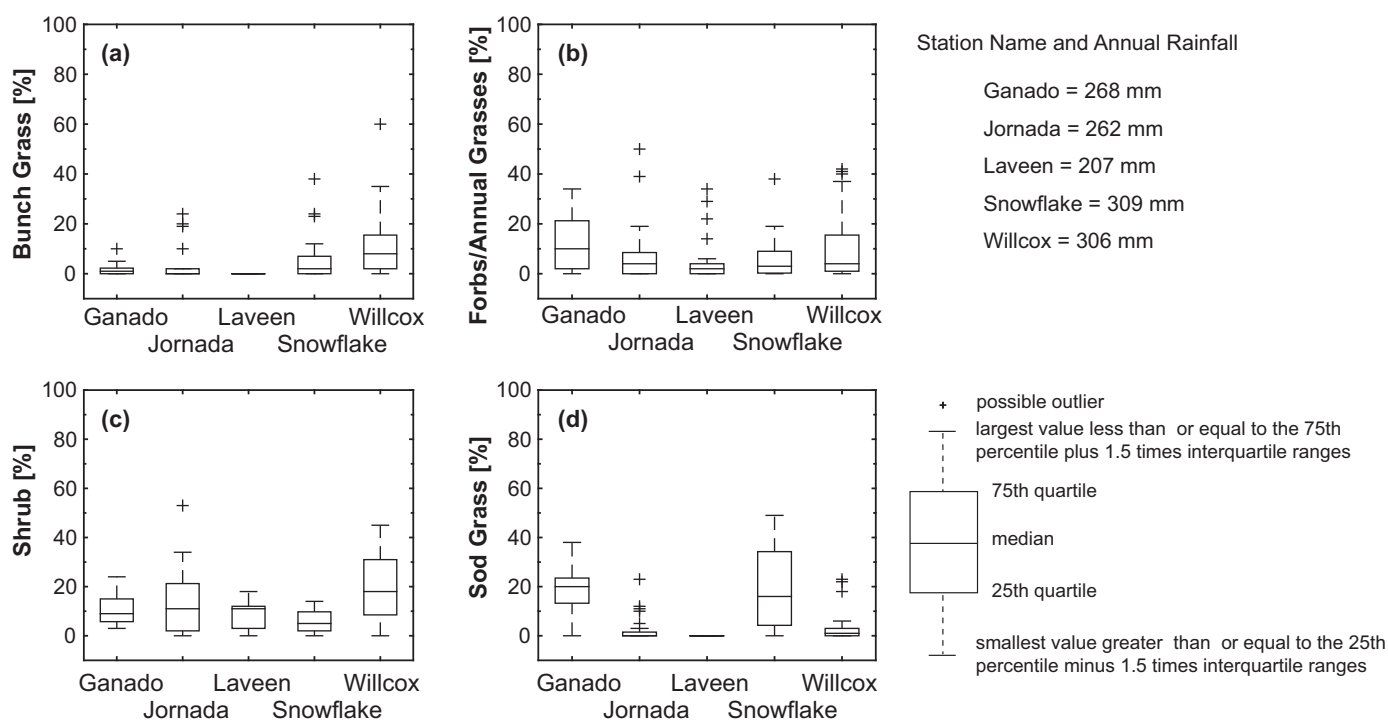


Figure 4. Distributions of foliar cover grouped by the five weather stations. (a) Bunchgrass, (b) forbs/annual grasses, (c) shrub, and (d) sodgrass for the NRI points.

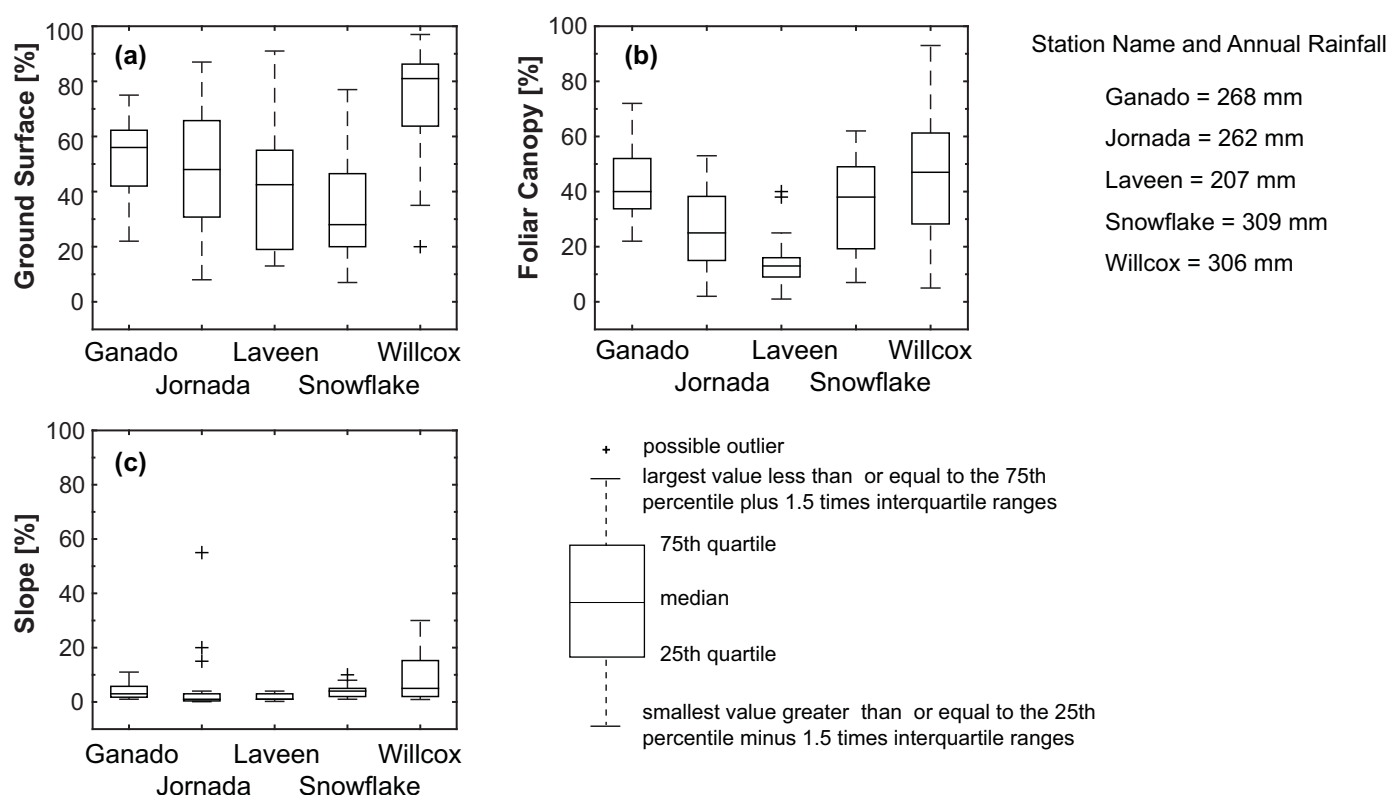


Figure 5. Distributions of total surface ground cover and foliar cover grouped by the five weather stations, and slope gradient of each NRI points classified based on the weather station's radius of influence.

However, based on Moriasi et al. (2007) *PBIAS* criterion, the RHEM performance can be evaluated for runoff volume and peak runoff as “very good” if $PBIAS < \pm 10$, “good” if $\pm 10 \leq PBIAS \leq \pm 15$, and “satisfactory” if $\pm 15 < PBIAS \leq \pm 25$, and for sediment yield can be evaluated as “good” if $PBIAS < \pm 15$. These criteria suggest that RHEM V2.3 can be evaluated as “very good” for runoff volume, “satisfactory” for peak runoff, and “very good” for sediment yield.

Positive *PBIAS* values indicate model underestimation bias, and negative values indicate overestimation bias (Gupta et al., 1999). An examination of Figure 6a indicates that the model performance for runoff volume prediction is poor with small events and improves with large events, which is common for models (Nearing, 2000). Furthermore, Figure 6b shows strong under prediction of peak runoff among nine runoff events, whereas sediment yield is in general over predicted for the small events in Figure 6c.

On the basis of the criteria for assessing goodness of fit of the model reported in Table 6 and the 1:1 line in Figure 6, it is reasonable to conclude that RHEM V2.3 performed reasonably well for the data from Lucky Hills.

4.2. Model Calibration

The calibration process was carried out using PEST; therefore, each calibrated parameter had a different value for different rainfall events on LH106. For most events, parameters were calibrated within eight iterations,

with a maximum number of 15 iterations. NSE for cumulative runoff volume ranges from 0.85 to 0.99 with a mean of 0.96, as there are 10 runoff data points and three calibrated parameters per event in the hydrology component of RHEM. The RHEM calibration produced the following average values of the overland flow parameters: total friction factor $f_t = 3.10$ (dimensionless), $K_e = 6.26$ (mm h^{-1}), and net capillary drive $C_d = 90$ (mm). The calculated parameters by the parameter estimation equations were as follows: total friction factor

Table 5
RHEM V2.3 Parameter Values for Lucky Hills 106

Parameters	Symbol	Units	Value
Total friction factor	f_t	Dimensionless	5.50
Effective saturated hydraulic conductivity	K_e	(mm h^{-1})	5.03
Splash and sheet erodibility coefficient	K_{ss}	($\text{kg m}^{-3.644} \text{s}^{0.644}$)	1366
Concentrated flow erodibility coefficient	K_w	($\text{s}^2 \text{m}^{-2}$)	5.04×10^{-5}

Table 6
Model Performance Statistics for Lucky Hills 106

Evaluation criteria	Runoff volume	Peak runoff	Sediment yield
RSR (dimensionless)	0.67	0.56	0.25
PBIAS (%)	−4	16	−7

$f_t = 5.50$ (dimensionless) and $K_e = 5.03$ (mm h^{-1}). The calibrated net capillary drive C_d value (90 mm) was smaller than that recommended in the KINEROS2 manual (127 mm) and reported by Rawls et al. (1982) for a sandy loam soil texture class.

The calibration of K_{ss} for each soil erosion event using PEST was achieved as follows. Total friction factor, effective saturated hydraulic conductivity, capillary drive, and concentrated flow erodibility

remained fixed for every calibration run. For most events K_{ss} was calibrated within three or five iterations. NSE for cumulative soil loss ranges from 0.81 to 0.96 with a mean of 0.90. The mean calibrated K_{ss} was 2089 ($\text{m}^2 \text{s}^{-2}$), which is higher than the value estimated by the equations proposed by Al-Hamdan et al. (2017) as reported in Table 5. The minimum, maximum, and average values for the calibrated parameters are presented in Table 7.

4.3. Performance Improvement From RHEM V1.0 to RHEM V2.3

The improvement made in model efficiency for the Lucky Hills site was 76% in comparison with the previous model version RHEM V1.0, especially with respect to low sediment yield simulation as shown by the NSE values in Figure 7.

The system of parameter estimation equations for RHEM V1.0 was developed by Nearing et al. (2011), and used the WEPP-IRWET rangeland dataset that contains measurements of simulated rainfall, runoff, and sediment discharge and soil and plant properties on 204 plots from 49 rangeland sites distributed across 15 western states. In all studies, the rotating-boom rainfall simulator (Swanson, 1965) was used to simulate rainfall for 30 min with an intensity of 60 mm/h.

Al-Hamdan et al. (2017) used the same WEPP-IRWET rangeland dataset for developing the new erodibility parameter equations in RHEM V2.3, but also used data for validation from independent rainfall simulation experiments conducted by the USDA-ARS Northwest Watershed Research Center, Boise, Idaho (Moffet et al., 2007; Pierson et al., 2007, 2009, 2010, 2013; Williams et al., 2014a). These experiments were conducted using a Colorado State University type rainfall simulator (Holland, 1969) consisting of multiple stationary sprinkler nozzles elevated 3.05 m above the ground surface (Pierson et al., 2007, 2009, 2010, 2013).

As a comparison, we followed the procedure outlined in Nearing et al. (2011) for estimating RHEM V1.0 parameter values for LH106. The computed effective saturated hydraulic conductivity and the splash and sheet erodibility coefficient are as follows: $K_e = 4.76 \text{ mm h}^{-1}$ and $K_{ss} = 1096$ ($\text{kg m}^{-3.644} \text{s}^{0.644}$), respectively. The RHEM V2.3 effective saturated hydraulic conductivity value is 5% greater than the RHEM V1.0; however, the RHEM V1.0 K_{ss} value is 25% smaller than the RHEM V2.3: $K_{ss} = 1366$ ($\text{kg m}^{-3.644} \text{s}^{0.644}$).

Al-Hamdan et al. (2017) employed piecewise (segmented) regression analysis where two continuous relationships between the log-transformed erodibility and the independent variables were fitted to improve the linear relationship. The piecewise regression analysis revealed that the best two-piece regression occurs

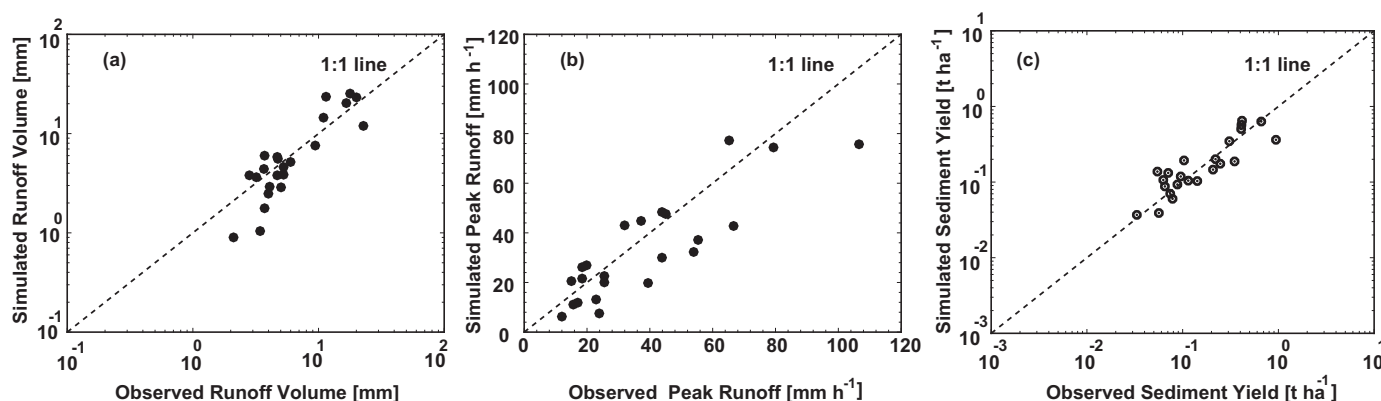


Figure 6. Comparison between observed and simulated results for each rainfall-runoff event at Lucky Hills 106: (a) runoff volume, (b) peak runoff, and (c) sediment yield. The parameters for these simulations were based on the RHEM V2.3 parameter estimation equations.

Table 7
Minimum, Maximum, and Average Values for the Calibrated Parameters

Parameter	Min	Max	Average
f_t (dimensionless)	0.96	19.62	3.10
K_e (mm h ⁻¹)	1.3	12.23	6.26
C_d (mm)	70	110	90
K_{ss} (m ² s ⁻²)	800	6240	2089

and K_{co} , estimated using equation (23), as the indicators of erodibility factor in RHEM, works reasonably well for this case. Splash and sheet and shallow concentrated flow erosion were observed on the hillslope, and the simulated contributions to sediment delivery from splash and sheet were 60% and 40% from shallow concentrated flow.

4.4. Model Application Using NRI Data

This section reports a case study of application of the model on a number of sites to assess the simulated effects of ground cover on total friction factor (f_t), estimated using equation (18), effective saturated hydraulic conductivity (K_e), estimated using equation (17), splash and sheet erodibility factor (K_{ss}), estimated using equations (19–22), and concentrated flow erodibility factor (K_{co}), as well as the effect of foliar cover and ground cover on sediment yield.

To investigate these effects, the model was applied to the 124 NRI points. The RHEM V2.3 model was run for a 300 year synthetic rainfall sequence generated by CLIGEN V5.3 (Nicks et al., 1995) based on the statistics of historic rainfall at each climate station. This is the default setup for running RHEM within the user interface.

The associations between ground cover and $\log_{10}(f_t)$ and K_e are shown in Figure 8, and the associations between ground cover and K_{ss} and K_{co} are shown in Figure 9. They provide a basis for evaluating the

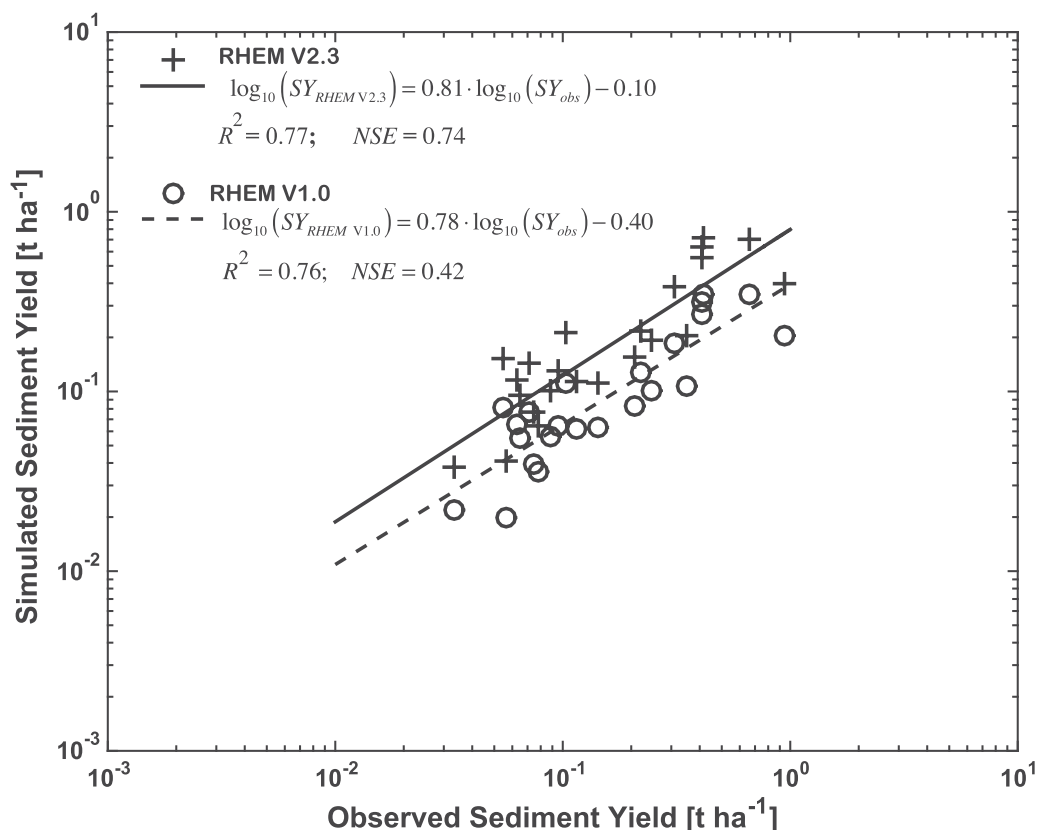


Figure 7. Simulated versus observed sediment yield showing model performance indicated by the NSE values on LH106 by RHEM V2.3 and RHEM V1.0 models.

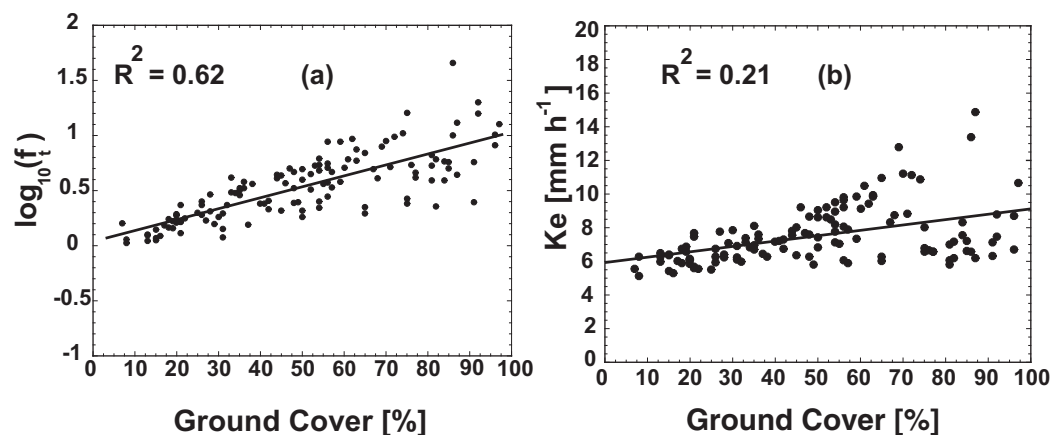


Figure 8. The relationships between ground cover and total friction factor (f_t), and effective saturated hydraulic conductivity (K_e); (a) strong positive linear correlation between ground cover and $\log_{10}(f_t)$, (b) moderate linear correlation between ground cover and K_e .

behavior of the parameter estimation equations. That is, $\log_{10}(f_t)$ increased with increasing ground cover as shown in Figure 8a, the strong positive correlation coefficient ($r = 0.79$, $p < 0.05$), suggesting that the parameter estimation equation to predict total friction roughness was not affected by outliers or small departures from model assumptions. For example, a slope gradient of 55% was reported in one NRI plot as shown in Figure 5c. Similarly, we expected that K_e would increase with increased litter cover and basal area cover as shown in Figure 8b. The spread of K_e around 80% ground cover, with the moderate correlation coefficient ($r = 0.46$, $p < 0.05$), suggests that the parameter estimation equation for predicting K_e for a sandy loam soil texture class was not affected by small departures from model assumptions. The rate of rapidly increasing K_{ss} starts at about 45% ground cover; this threshold value is consistent with several studies that concluded that ground cover should be maintained above a critical threshold of ~ 50 – 60% to protect the soil surface adequately (Gifford, 1985; Pierson et al., 2009, 2010, 2013; Weltz et al., 1998). A strong negative Spearman correlation coefficient ($\rho = -0.71$, $p < 0.05$) and a fitted decaying exponential model ($R^2 = 0.82$, $p < 0.05$) to the data shown in Figure 9a confirm the expected decreasing monotonic trend between ground cover and K_{ss} . The NRI point with 55% slope gradient did not appear to cause an adverse effect on the correlation coefficient and fitted decaying exponential model. Furthermore, a strong negative Spearman correlation coefficient ($\rho = -0.94$, $p < 0.05$) and a fitted decaying exponential model ($R^2 = 0.87$, $p < 0.05$) to the data shown in Figure 9b confirms the expected decreasing monotonic trend between ground cover and K_{co} .

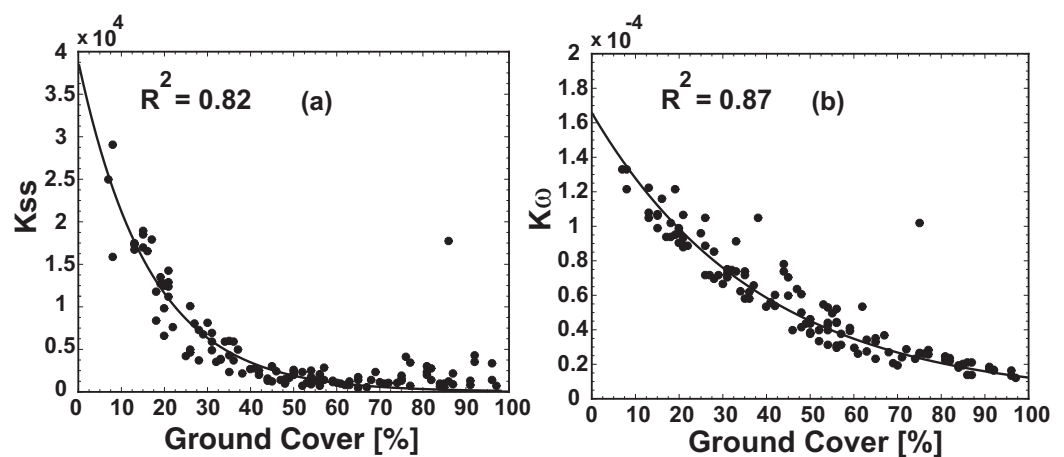


Figure 9. The relationships between ground cover and splash and sheet erodibility coefficient (K_{ss}) and concentrated flow erodibility coefficient (K_{co}); (a) strong Spearman rank correlation coefficient between ground cover and K_{ss} , (b) strong Spearman rank correlation coefficient between ground cover and K_{co} .

An examination of Figure 9b shows a point with a high K_{co} value [1.02×10^{-4} ($s^2 m^{-2}$)] at 75% ground cover. Ground cover at this plot is characterized by 0% rock cover, 14% litter cover, and 46% biological soil crust cover (see Figure 3b). The equation to estimate K_{co} , equation (23), does not account for biological soil crust cover; thus, sediment detachment in concentrated flow will occur despite the good protection by the soil crust cover.

The impact of biological soil crusts on infiltration rates and soil erosion is poorly understood and often contradictory. Biological soil crusts can reduce infiltration rates and increase soil erosion by blocking flow through macropores or they may enhance porosity and infiltration rates by increasing water-stable aggregates and surface roughness (Eldridge & Koen, 1998; Loope & Gifford, 1972; West, 1991). The exact response on runoff and soil erosion is a function of site disturbance and level of development of the biological soil crusts (Belnap et al., 2013). When studies are evaluated based on biological crust type and utilizing naturally occurring differences among crust types, results indicate that biological crusts in hyper-arid regions reduce infiltration and increase runoff, biological soil crusts have mixed effects in arid regions, and increase infiltration and reduce runoff in semiarid cool regions. Most research has shown that intact biological soil crusts are effective at reducing soil erosion and transport of soils and associated contaminants (Belnap, 2006). Additional research is required before the role that biological soil crusts play in altering detachment and transport of soils and salts (dissolution of salt crusts by efflorescence) is fully understood. While mechanisms of concentrated flow detachment are well understood, prediction of sediment delivery is complicated because none of these studies evaluated deposition processes on sites with biological soil crusts.

On rangelands, plant growth forms, litter, and basal cover, and numerous soil properties have been correlated with various hydrologic criteria such as infiltration, runoff, and erosion. Regarding the influence of litter and basal cover on percent runoff, defined as the ratio of runoff to precipitation, we found a strong negative linear correlation ($r = -0.70$, $p < 0.05$) with litter as depicted in Figure 10a. Two distinct patterns of percent runoff emerged as a function of annual rainfall amount observed at the Ganado and Willcox weather stations. Both weather stations' area of influence had similar average amounts of litter cover percent (Ganado: mean = 34% and Willcox: mean = 31%), but distinct annual rainfall regimes (Ganado: 268 mm and Willcox: 306 mm). Further, the Ganado's area of influence was characterized as sod grasses (mean = 19%) and forb/annual grasses (mean = 12%), and the Willcox's area was characterized by a combination of shrub (mean = 19%), bunch grasses (12%), and forb/annual grasses (mean = 11%). The Laveen weather station has the lowest annual rainfall amount (207 mm), the lowest litter cover percent (16%), and was mainly shrub-forb/annual grasses-dominated (mean = 9% and mean = 6%, respectively).

A moderate negative relationship was found between basal cover and percent runoff, and is depicted in Figure 10b. Although no patterns emerged in this relation, the model was able to capture the influence of basal dynamics by showing a negative trend.

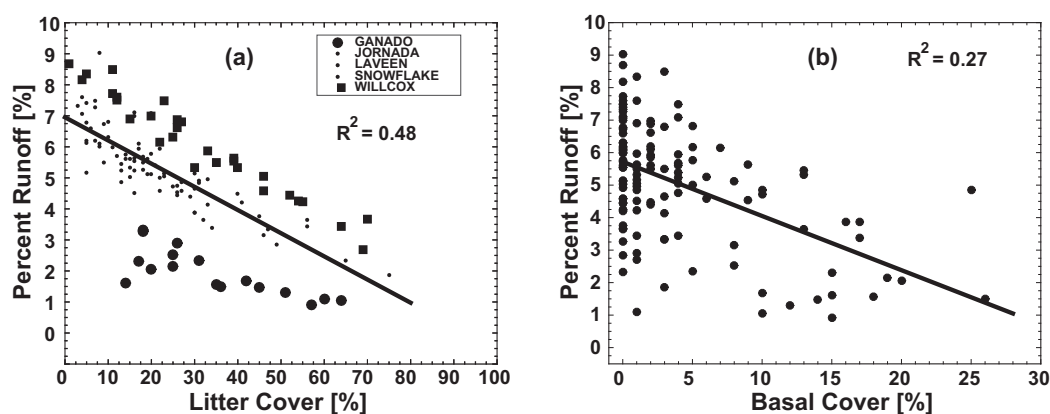


Figure 10. Runoff as a percent of precipitation showing the negative relationship with (a) litter cover percent and (b) basal cover percent.

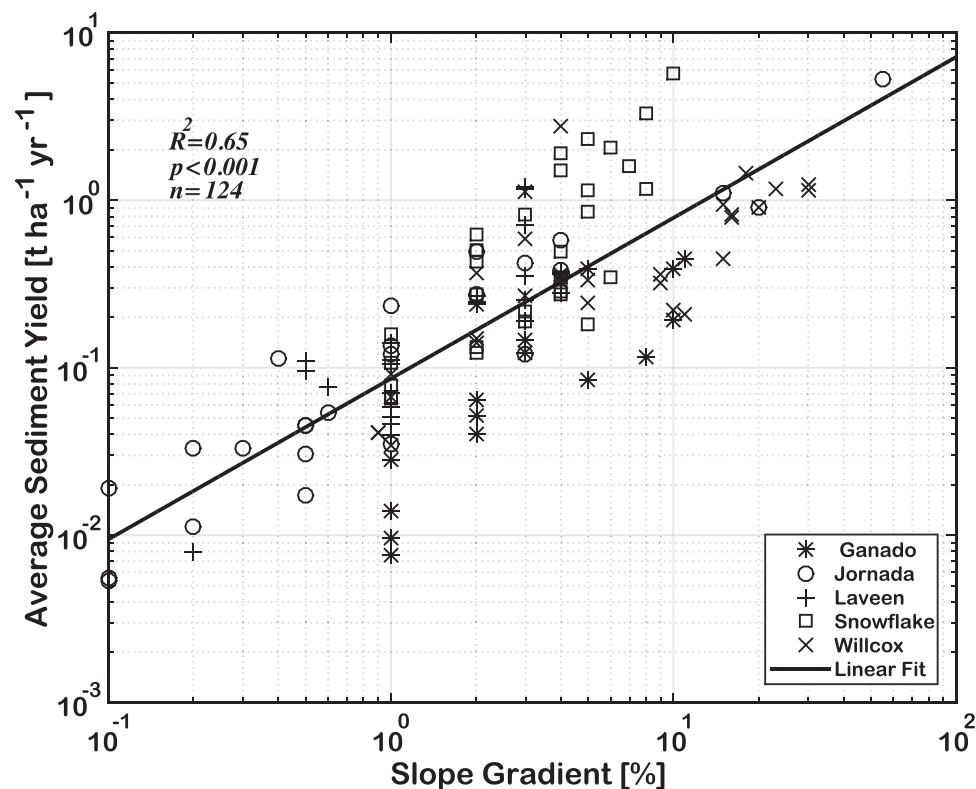


Figure 11. Relationship between average annual sediment yield and slope gradient for the 124 NRI points affected by five precipitation regimes.

We also investigated the effect of slope steepness on sediment yield. Transport capacity increases as flow rate and slope steepness increase. The parameter estimation equations for calculating concentrated flow width, hydraulic roughness, and splash and sheet erodibility depend on the geometry of the upland area as described by the surface slope steepness. Figure 11 shows the graph of annual sediment yield versus slope steepness for the 124 NRI points.

Sediment yield and slope gradient are strongly correlated ($R^2 = 0.65$; $p < 0.001$) with a large variability around the 1% and 3% slope gradient interval, 60% of the points falls within this percent interval. The variability represented by the coefficient of variation (CV) in slope gradient, litter, rock and annual sediment yield of the five rainfall regimes is reported in Table 8. The variability in rock cover on the Ganado, Jornada Experimental Range, Laveen and Snowflake and slope gradient on the Jornada Experimental Range contribute to some extent to the large variability in annual sediment yield. Moreover, a coefficient of variation less than 1 is considered to be low-variance, consequently, the variability in simulated sediment yield was less affected by the dispersion in litter cover, and slope gradient, except for the Jornada Experimental Range.

Table 8
Variation of Mean and CV in Slope Steepness, Litter, Rock, and Annual Sediment Yield for the 124 NRI Points

Weather Station	N	Rainfall (mm)	Slope		Litter		Rock		Annual sediment yield	
			Mean (%)	CV	Mean (%)	CV	Mean (%)	CV	Mean (t ha^{-1})	CV
Ganado	17	268	4.18	0.83	34.35	0.47	3.94	2.66	0.16	0.95
Jornada Exp	25	262	4.64	2.48	23.96	0.73	22.64	1.06	0.42	2.51
Laveen	22	207	1.81	0.67	16.00	0.91	21.18	1.01	0.27	1.24
Snowflake	31	309	3.74	0.63	24.00	0.49	2.35	3.45	0.88	1.36
Willcox	29	306	9.10	0.96	31.45	0.62	39.97	0.73	0.59	1.01

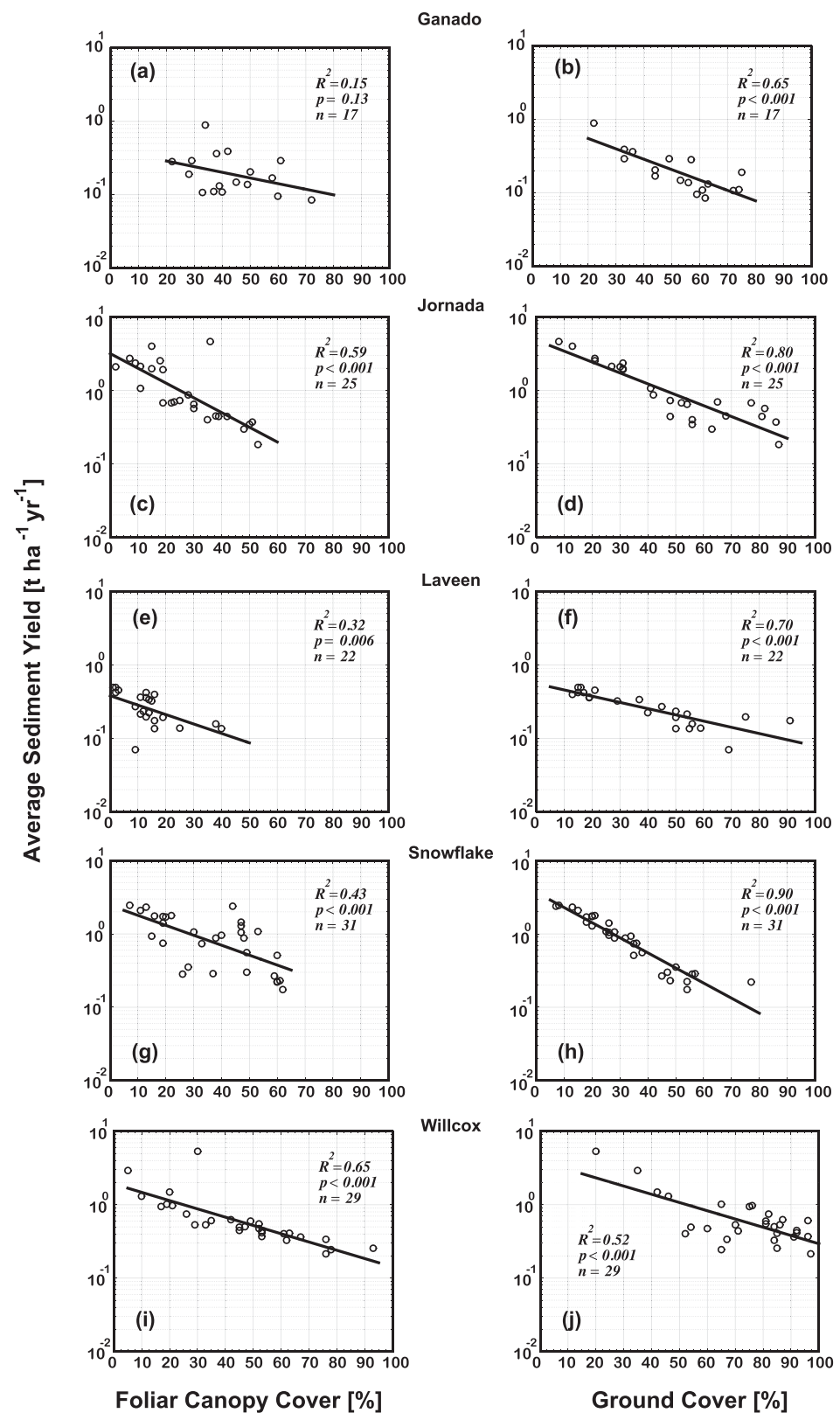


Figure 12. Association between predicted average sediment yield and foliar cover and ground cover for the five precipitation regimes.

We estimated the correlation coefficient to measure the strength of association between average annual sediment yield and the variables foliar cover and ground cover, and grouped these by weather stations. Since the variability in sediment yield for each precipitation regime was large, sediment yield was normalized to fit a single equation to the sediment yield, foliar cover and ground cover data from each precipitation regime. The mean slope gradient percent of NRI points within each precipitation regime represented by the five weather stations shown in Table 8 was selected for the normalization. The results are shown in Figure 12.

The strength of the association between average annual sediment yield and foliar and ground cover is moderate to strong; the correlation coefficient varied from -0.39 to -0.81 and -0.72 to -0.95 for foliar and ground cover, respectively. When shrub is the dominant plant form, the relationship between sediment yield and foliar cover is the strongest as shown in Figures 12c and 12i. Conversely, the weakest relationship between sediment yield and foliar cover appears to be when sod or forbs are the dominant plant forms as indicated in Figures 12a, 12e, and 12g. The area covered by the Ganado weather station has the fewest number of NRI points ($n = 17$) and is dominated by forbs/annual grasses and sod grasses. The low number of NRI points and the high variability in these grasses, as shown in Figures 4b and 4d, can be attributed to the fact that only 15% of the variability between the annual sediment yield and foliar cover can be accounted for. When litter and rock cover are the most dominant variables, the association between average annual sediment yield and ground cover is very strong, as indicated in Figures 12b, 12d, 12f, 12h, and 12j.

These results suggest that low yearly sediment yield, in general, is not well described by foliar cover. We found that the association is stronger with ground cover than with foliar cover, which is expected (e.g., Nearing et al., 2005). The results suggest that ground cover, in general, is more highly associated with yearly sediment yield than foliar cover.

5. Conclusions

In this article, we presented an improved version of the RHEM model (RHEM V2.3). This model was developed to fill the need for a process-based rangeland erosion model that can function as a practical tool for quantifying runoff and erosion rates specific to rangelands with varied life/growth form traits and composition to provide runoff and soil loss prediction capacity for rangeland management and research.

The improvement made in model efficiency is significant in comparison with the original version RHEM V1.0 when the new equations for estimating K_{ss} , equations (19)–(22), and K_{er} , equation (23), are used, especially with respect to low-sediment yield simulation. The model with the new parameterization equations works reasonably well as long as concentrated flow paths function only for transport of the splash and sheet-generated sediment, as opposed to functioning as the main sediment source. Splash and sheet and shallow concentrated flow erosion processes were observed on the Lucky Hills 106 subwatershed with a mild slope gradient (8%); contribution to sediment delivery from splash and sheet was 60% and 40% from shallow concentrated flow. On the basis of the *PBIAS* values, the model shows strong under prediction of peak runoff and over prediction of small events of sediment yield. According to the *NSE* criterion, the performance of the RHEM V2.3 model with the new erodibility equations at the hillslope scale was superior to RHEM V1.0.

The parameter values calculated with the RHEM V2.3 parameter estimation equations fell within the lowest and highest calibrated values of each parameter. The ability of the parameter estimation equations to adequately produce parameter values for the application of RHEM on a small watershed suggest that the model is suited for small subwatersheds, provided that gully erosion is not the main active process in the watershed.

The analysis of the 124 NRI field study points in Arizona and New Mexico suggests that the parameter estimation equations conveyed coherent information to the model. That is, moderate positive correlation coefficients were achieved between ground cover and total friction factor, and effective hydraulic conductivity. In contrast, strong negative correlation coefficients were found between ground cover and splash and sheet erodibility, and concentrated flow erodibility. Likewise, moderate and strong negative correlation coefficients were found between litter cover and basal cover percent and percent runoff. Furthermore, moderate and strong negative correlation coefficients were found between foliar cover and ground cover and

sediment yield. In general, the model results are more sensitive to ground cover than to foliar cover, which is a product of the structure of the parameter estimation equations. This is consistent with our understanding of the basic processes of soil erosion, largely because of shear stress partitioning, and of most soil erosion models.

Evaluation of the model predictions undertaken in this study demonstrates that RHEM V2.3 produces satisfactory results when simulating large flow and soil erosion events, but a greater degree of uncertainty is associated with predictions of small runoff and soil erosion events. Despite the advancement of modeling splash and sheet and concentrated flow, as represented in RHEM, future work is still needed for improving the prediction of erosion processes. While the model can simulate detachment rate in concentrated flow, it does not model or predict concentration flow formation or concentrated flow initiation. However, the model does provide a logistic function to estimate the probability of overland flow to become concentrated flow on rangeland. Knowledge on the feedback between splash and sheet and concentrated flow processes is needed to further improve hydrology and erosion modeling on rangeland.

Acknowledgments

The authors wish to thank the U.S. Department of Agriculture for funding of this project. We thank the field staff of the Walnut Gulch Experimental Watershed and scientists and staff of the USDA-ARS, Southwest Watershed Research Center for their dedication and effort that made the collection and use of these data possible. All data for precipitation, runoff, sediment, and soil moisture used in this study are available for public download through the USDA-ARS Southwest Watershed Research Center at <http://www.tucson.ars.ag.gov/dap/>. Professor Sean J. Bennett and two anonymous reviewers are gratefully acknowledged for their constructive comments that helped to substantially improve the paper.

References

- Al-Hamdan, O. Z., Hernandez, M., Pierson, F. B., Nearing, M. A., Williams, C. J., Stone, J. J., . . . Wetz, M. A. (2015). Rangeland hydrology and erosion model (RHEM) enhancements for applications on disturbed rangelands. *Hydrological Processes*, 29(3), 445–457.
- Al-Hamdan, O. Z., Pierson, F. B., Nearing, M. A., Stone, J. J., Williams, C. J., Moffet, C. A., . . . Wetz, M. A. (2012a). Characteristics of concentrated flow hydraulics for rangeland ecosystems: Implications for hydrologic modeling. *Earth Surface Process and Landforms*, 37, 157–168.
- Al-Hamdan, O. Z., Pierson, F. B., Nearing, M. A., Williams, C. J., Hernandez, M., Boll, J., . . . Spaeth, K. (2017). Developing a parameterization approach for soil erodibility for the Rangeland Hydrology and Erosion Model (RHEM). *Transactions of the ASABE*, 60(1), 85–94.
- Al-Hamdan, O. Z., Pierson, F. B., Nearing, M. A., Williams, C. J., Stone, J. J., Kormos, P. R., . . . Wetz, M. A. (2012b). Concentrated flow erodibility for physically based erosion models: Temporal variability in disturbed and undisturbed rangelands. *Water Resources Research*, 48, W07504. <https://doi.org/10.1029/2011WR011464>
- Al-Hamdan, O. Z., Pierson, F. B., Nearing, M. A., Williams, C. J., Stone, J. J., Kormos, P. R., . . . Wetz, M. A. (2013). Risk assessment of erosion from concentrated flow on rangelands using overland flow distribution and shear stress partitioning. *Transactions of the ASABE*, 56(2), 539–548.
- Belnap, J. (2006). The potential roles of biological soil crusts in dryland hydrologic cycles. *Hydrological Processes*, 20, 3159–3178.
- Belnap, J., Wilcox, B. P., Van Scoyoc, M. W., & Phillips, S. L. (2013). Successional stage of biological soil crusts: An accurate indicator of ecophysiological condition. *Ecophysiology*, 6, 474–482.
- Bennett, J. P. (1974). Concepts of mathematical modeling of sediment yield. *Water Resources Research*, 10(3), 485–492.
- Bulygina, N. S., Nearing, M. A., Stone, J. J., & Nichols, M. H. (2007). DWEPP: A dynamic soil erosion model based on WEPP source terms. *Earth Surface Processes and Landforms*, 32, 998–1012.
- Davenport, D. W., Breshears, D. D., Wilcox, B. P., & Allen, C. D. (1998). Viewpoint: Sustainability of piñon-juniper ecosystems a unifying perspective of soil erosion threshold. *Journal of Range Management*, 51, 231–240.
- Doherty, J. (2015). *Calibration and uncertainty analysis for complex environmental models*. Brisbane, Australia: Watermark Numerical Computing. Fort Collins, CO: U.S. Department of Agriculture.
- Dortignac, E. J., & Love, L. D. (1961). *Infiltration studies on ponderosa pine ranges of Colorado* (Rocky Mountain Forest and Range Exp. Sta., Pap. 59, 34 p.). Fort Collins, CO: U.S. Department of Agriculture.
- Duan, N. (1983). Smearing estimates: A nonparametric retransformation method. *Journal of the American Statistical Association*, 78(383), 605–610.
- Eldridge, D. J., & Koen, T. B. (1998). Cover and floristics of microphytic soil crusts in relation to indices of landscape health. *Plant Ecology*, 137, 101–114.
- Fair, G. M., & Geyer, J. C. (1954). *Water supply and wastewater disposal* (973 pp.). New York, NY: John Wiley.
- Flanagan, D. C., and Nearing, M. A. (Eds.). (1995). USDA Water Erosion Prediction Project hillslope profile and watershed model documentation (NSERL Rep. 10). West Lafayette, ID: USDA-ARS National Soil Erosion Research Laboratory.
- Foltz, R. B., Rhee, H., & Elliot, W. J. (2008). Modeling changes in rill erodibility and critical shear stress on native surface roads. *Hydrological Processes*, 22, 4783–4788.
- Foster, G. R. (1982). Modeling the erosion process, In C. T. Hann, H. P. Johnson, & D. L. Brakensiek (Eds.), *Hydrologic modeling of small watersheds, ASAE Monograph* (Vol. 5, pp. 297–360). St. Joseph, MI: American Society of Association Executives.
- Gifford, G. F. (1985). Cover allocation in rangeland watershed management. In E. B. Jones & T. J. Ward (Eds.), *Watershed management in the eighties* (pp. 23–31). New York, NY: American Society of Civil Engineers.
- Goodrich, D. C., Bums, I. S., Unkrich, C. L., Semmens, D. J., Guertin, D. P., Hernandez, M., . . . Levick, L. R. (2012). KINEROS2/AGWA: Model use, calibration, and validation. *Transactions of the ASABE*, 55(4), 1561–1574.
- Goodrich, D. C., Keefer, T. O., Unkrich, C. L., Nichols, M. H., Osborn, H. B., Stone, J. J., & Smith, J. R. (2008). Long-term precipitation database, Walnut Gulch Experimental Watershed, Arizona, United States. *Water Resources Research*, 44, W05504. <https://doi.org/10.1029/2006WR005782>
- Green, W. H., & Ampt, A. G. (1911). Studies of soil physics. Part I—The flow of air and water through soils. *Journal of the Agricultural Science*, 4, 1–24.
- Gupta, H. V., Sorooshian, S., & Yapo, P. O. (1999). Status of automatic calibration for hydrologic models: Comparison with multilevel expert calibration. *Journal of Hydrologic Engineering*, 4(2), 135–143.
- Havstad, K. M., Peters, Allen-Diaz, D. B., Bestelmeyer, B., Briske, T. D., Brown, J., Brunson, L. M., . . . Huntsinger, L. (2009). The western United States rangelands, a major resource. In W. F. Wedin & S. L. Fales (Eds.), *Grassland, quietness and strength for a New American Agriculture* (Chapter 5, pp. 75–93). Madison, WI: American Society of Agronomy.

- Hernandez, M., Nearing, M. A., Pierson, F. B., Williams, C. J., Spaeth, K. E., & Weltz, M. A. (2016, 17–22 July). A risk-based vulnerability approach for rangeland management. In *Proceedings of the 10th international rangeland congress, the future management of grazing and wild lands in a high tech world*, (pp. 1014–1015). Saskatoon, SK.
- Hernandez, M., Nearing, M. A., Stone, J. J., Armendariz, G., Pierson, F. B., Al-Hamdan, O. Z., . . . & Goodrich, D. C. (2015, 31 January–6 February). Web-based rangeland hydrology and erosion model. In *Proceedings of the 68th range management annual meeting*, Sacramento, CA.
- Hernandez, M., Nearing, M. A., Stone, J. J., Pierson, F. B., Wei, H., Spaeth, K. E., . . . Goodrich, D. C. (2013). Application of a rangeland soil erosion model using NRI data in southeastern Arizona. *Journal of Soil and Water Conservation*, 68(6), 512–525.
- Herrick, J. E., Wills, S., Karl, J., & Pyke, D. (2010). *Terrestrial indicators and measurements: Selection process and recommendations*. Las Cruces, NM: U.S. Department of Agriculture. Final Report. Retrieved from https://jornada.nmsu.edu/files/AIM_Terrestrial_Indicators_Selection.pdf
- Holland, M. E. (1969). *Design and testing of a rainfall system* (CER69–70. MEH 21). Ft Collins, CO: Colorado State University Experiment Station.
- Interagency Rangeland Water Erosion Team & National Rangeland Study Team (1998). *Interagency Rangeland Water Erosion Project report and state data summaries* (NWRC 98-1). Boise, Idaho: USDA-ARS Northwest Watershed Research Center.
- Kalin, L., Govindaraju, R. S., & Hantush, M. M. (2004). Development and application of a methodology sediment source identification. I: Modified unit sedimentograph approach. *Journal of Hydrologic Engineering*, 9(3), 184–193.
- Keefer, T. O., Moran, M. S., & Paige, G. B. (2008). Long-term meteorological and soil hydrology database, Walnut Gulch Experimental Watershed, Arizona, United States. *Water Resources Research*, 44, W05S07. <https://doi.org/10.1029/2006WR005708>
- Keefer, T. O., Renard, K. G., Goodrich, D. C., Heilman, P., & Unkrich, C. L. (2015). Quantifying extreme precipitation events and their hydrologic response in southeastern Arizona. *Journal of Hydrologic Engineering*, 21(1), 1–10. [https://doi.org/10.1061/\(ASCE\)HE.1943-5584.0001270](https://doi.org/10.1061/(ASCE)HE.1943-5584.0001270)
- Lane, L. J., Hernandez, M., & Nichols, M. H. (1997). Processes controlling sediment yield from watersheds as functions of spatial scale. *Environmental Modelling and Software*, 12(4), 355–369.
- Loope, W. L., & Gifford, G. F. (1972). Influence of a soil microfloral crust on select properties of soils under pinyon-juniper in southeastern Utah. *Journal of Soil and Water Conservation*, 27, 164–167.
- Ludwig, J. A., Wilcox, B. P., Breshears, D. D., Tongway, D. J., & Imeson, A. C. (2005). Vegetation patches and runoff erosion as interacting ecohydrological processes in semiarid landscapes. *Ecology*, 86(2), 288–297.
- Meeuwig, R. O. (1970). Infiltration and soil erosion as influenced by vegetation and soil in northern Utah. *Journal of Range Management*, 23, 185–189.
- Moffet, C. A., Pierson, F. B., Robichaud, P. R., Spaeth, K. E., & Hardegree, S. P. (2007). Modeling soil erosion on steep sagebrush rangeland before and after prescribed fire. *Catena*, 71(2), 218–228.
- Moriasi, D. N., Arnold, J. G., Van Liew, M. W., Bingner, R. L., Harmel, R. D., & Veith, T. L. (2007). Model evaluation guideline for systematic quantification of accuracy in watershed simulations. *Transactions of the ASAE*, 50(3), 885–900.
- Müller, K., Smith, R. E., James, T. K., Holland, P. T., & Rahman, A. (2003). Prediction of field atrazine persistence in an allophanic soil with Opus2. *Pest Management Science*, 60(5), 447–458.
- Nash, J. E., & Sutcliffe, J. V. (1970). River flow forecasting through conceptual models. Part I—A discussion of principles. *Journal of Hydrology*, 10(3), 282–290.
- Nearing, M. A. (2000). Evaluating soil erosion models using measured plot data: Accounting for variability in the data. *Earth Surface Process and Landforms*, 25, 1035–1043.
- Nearing, M. A., & Hairsine, P. B. (2011). The future of soil erosion modelling, In R. P. Morgan & M. A. Nearing (Eds.), *Handbook of erosion modelling*. Chichester, UK: Wiley-Blackwell Publishers.
- Nearing, M. A., Jetten, V., Baffaut, C., Cerdan, O., Couturier, A., Hernandez, M., . . . van Oost, K. (2005). Modeling response of soil erosion and runoff to changes in precipitation and cover. *Catena*, 61(2–3), 131–154.
- Nearing, M. A., Nichols, M. H., Stone, J. J., Renard, K. G., & Simanton, J. R. (2007). Sediment yields from unit-source semi-arid watersheds at Walnut Gulch. *Water Resources Research*, 43, W06426. <https://doi.org/10.1029/2006WR005692>
- Nearing, M. A., Norton, L. D., Bulgakov, D. A., Larionov, G. A., West, L. T., & Dontsova, K. M. (1997). Hydraulics and erosion in eroding rills. *Water Resources Research*, 33(4), 865–876.
- Nearing, M. A., Pruski, F. F., & O'neal, M. R. (2004). Expected climate change impacts on soil erosion rates: A review. *Journal of Soil and Water Conservation*, 59(1), 43–50.
- Nearing, M. A., Wei, H., Stone, J. J., Pierson, F. B., Spaeth, K. E., Weltz, M. A., . . . Hernandez, M. (2011). A rangeland hydrology and erosion model. *Transactions of the ASAE*, 54(3), 901–908.
- Nearing, M. A., Unkrich, C., Goodrich, D. C., Nichols, M. H., & Keefer, T. O. (2015). Temporal and elevation trends in rainfall erosivity on a 149km² watershed in a semi-arid region of the American Southwest. *International Soil and Water Conservation Research*, 3, 77–85. <http://doi.org/10.1016/j.iswcr.2015.06.008>
- Nichols, M. H., Nearing, M. A., Polyakov, V. O., & Stone, J. J. (2012). A sediment budget for a small semiarid watershed in southeastern Arizona, USA. *Geomorphology*, 180, 137–145. <https://doi.org/10.1016/j.geomorph.2012.10.002>
- Nicks, A. D., Lane, L. J., & Gander, G. A. (1995). Weather generator. In D. C. Flanagan & M. A. Nearing (Eds.), *USDA-water erosion prediction project: Hillslope profile and watershed model documentation* (Chapter 2, NSERL Rep. 10). West Lafayette, IN: USDA-ARS National Soil Erosion Research Laboratory.
- Nusser, S. M., & Goebel, J. J. (1997). The national resources inventory: A long-term multi-resource monitoring programme. *Environmental and Ecological Statistics*, 4(3), 181–204.
- Okin, G. S., las Heras, M. M-D., Saco, P. M., Throop, H. L., Vivoni, E. R., Parsons, A. J., . . . Eters, D. P. (2015). Connectivity in dryland landscapes: Shifting concepts of spatial interactions. *Frontiers in Ecology and the Environment*, 13, 20–27.
- Parlange, J.-Y., Lisle, I., Braddock, R. D., & Smith, R. E. (1982). The three-parameter infiltration equation. *Soil Science*, 133(6), 337–341.
- Pierson, F. B., Bates, J. D., Svejcar, T. J., & Hardegree, S. P. (2007). Runoff and erosion after cutting western juniper. *Rangeland Ecology & Management*, 60, 285–292.
- Pierson, F. B., Carlson, D. H., & Spaeth, K. E. (2002). Impacts of wildfire on soil hydrological properties of steep sagebrush-steppe rangeland. *International Journal of Wildfire*, 11, 145–151.
- Pierson, F. B., Moffet, C. A., Williams, C. J., Hardegree, S. P., & Clark, P. (2009). Prescribed-fire effects on rill and interrill runoff and erosion in a mountainous sagebrush landscape. *Earth Surface Processes and Landforms*, 34, 193–203.

- Pierson, F. B., Robichaud, P. R., Moffet, C. A., Spaeth, K. E., Hardegree, S. P., Clark, P. E., & Williams, C. J. (2008). Fire effects on rangeland hydrology and erosion in a steep sagebrush-dominated landscape. *Hydrological Processes*, 22, 2916–2929.
- Pierson, F. B., & Williams, C. J. (2016). *Ecohydrologic impacts of rangeland fire on runoff and erosion: A literature synthesis* (Gen. Tech. Rep. RMRS-GTR-351, 110 p.). Fort Collins, CO: U.S. Department of Agriculture, Forest Service, Rocky Mountain Research Station. Retrieved from <https://www.treesearch.fs.fed.us/pubs/52310>
- Pierson, F. B., Williams, C. J., Hardegree, S. P., Clark, P. E., Kormos, P. R., & Al-Hamdan, O. Z. (2013). Hydrologic and erosion responses of sagebrush steppe following juniper encroachment, wildfire, and tree cutting. *Rangeland Ecology & Management*, 66, 274–289.
- Pierson, F. B., Williams, C. J., Hardegree, S. P., Wertz, M. A., Stone, J. J., & Clark, P. E. (2011). Fire, plant invasions, and erosion events on western rangelands. *Rangeland Ecology & Management*, 64, 439–449.
- Pierson, F. B., Williams, C. J., Kormos, P. R., Hardegree, S. P., & Clark, P. E. (2010). Hydrologic vulnerability of sagebrush steppe following pinon and juniper encroachment. *Rangeland Ecology & Management*, 63, 614–629. <https://doi.org/10.2111/REM-D-09-00148.1>
- Puigdefabregas, J. (2005). The role of vegetation patterns in structuring runoff and sediment flux in drylands. *Earth Surface Processes and Landforms*, 30, 133–147.
- Ravi, S., Breshears, D. D., Huxman, T. E., & D'odorico, P. (2010). Land degradation in drylands: Interactions among hydrologic-aeolian erosion and vegetation dynamics. *Geomorphology*, 116, 236–245.
- Rawls, W. J., Brakensiek, D. L., & Saxton, K. E. (1982). Estimation of soil water properties. *Transactions of the ASAE*, 25(5), 1316–1320.
- Rawls, W. J., Brakensiek, D. L., Simanton, J. R., & Kho, D. (1990). Development of a crust factor for a Green Ampt model. *Transactions of the ASAE*, 33(4), 1224–1228.
- Rawls, W. L., Gimenez, D., & Grossman, R. (1998). Use of soil texture, bulk density, and slope of the water retention curve to predict saturated hydraulic conductivity. *Transactions of the ASAE*, 41, 983–988.
- Renard, K. G. (1980). Estimating erosion and sediment yield from rangelands. In C. W. Johnson & R. H. Hawkins (Eds.), *Proceedings of the ASCE Symposium on Watershed Management '80* (pp. 164–175). Boise, ID: Watershed Management Committee of the Water Resources Engineering Division.
- Renard, K. G., Nichols, M. H., Woolhiser, D. A., & Osborn, H. B. (2008). A brief background on the U.S. Department of Agriculture Agricultural Research Service Walnut Gulch Experimental Watershed. *Water Resources Research*, 44, W05S02. <https://doi.org/10.1029/2006WR005691>
- Robichaud, P. R., Ashmun, L. E., & Sims, B. (2010). Post-fire treatment effectiveness for hillslope stabilization (General Tech. Rep. RMRS-GTR-240). Fort Collins, CO: U.S. Department of Agriculture, Forest Service, Rocky Mountain Research Station.
- Rosentreter, R., Bowker, M., & Belnap, J. (2007). *A field guide to biological soil crusts of western U.S. drylands*. Denver, CO: U.S. Government Printing Office.
- Schaffner, M., Unkrich, C. L., & Goodrich, D. C. (2010). *Application of the KINEROS2 site specific model to south-central NY and northeast PA: Forecasting gaged and ungaged fast responding watersheds*. NWS Eastern Region Technical Attachment (2010-01). Retrieved from <http://www.weather.gov/media/erh/ta2010-01.pdf>
- Schoeneberger, P. J., Wysocki, D. A., Benham, E. C., & Soil Survey Staff (2012). Field book for describing and sampling soils, Version 3.0. Lincoln, NE: Natural Resources Conservation Service, National Soil Survey Center.
- Simanton, J. R., Osterkamp, W. R., & Renard, K. G. (1993, July). Sediment yield in a semiarid basin: Sampling equipment impacts. In R. F. Hadley & T. Mizuyama (Eds.), *Proceedings of the Yokohama, Japan Symposium, Sediment problems: Strategies for monitoring, prediction and control* (IAHS Publication Number 217, pp. 3–9). Wallingford, UK: International Association of Hydrological Sciences.
- Smith, R. E., Corradini, C., & Melone, F. (1993). Modeling infiltration for multi-storm runoff events. *Water Resources Research*, 29(1), 133–144.
- Smith, R. E., & Goodrich, D. C. (2000). Model for rainfall excess patterns on randomly heterogeneous areas. *Journal of Hydrologic Engineering*, 5(4), 355–362.
- Smith, R. E., Goodrich, D. C., Woolhiser, D. A., & Unkrich, C. L. (1995). KINEROS—A kinematic runoff and erosion model. In V. P. Singh (Ed.), *Computer models of watershed hydrology* (pp. 697–732). Highlands Ranch, CO: Water Resources Publications.
- Smith, R. E., & Parlange, J.-Y. (1978). A parameter-efficient hydrologic infiltration model. *Water Resources Research*, 14(3), 533–538.
- Spaeth, K. E. (1990). *Hydrologic and ecologic assessments of a discrete range site on the Southern High Plains* (Ph.D. dissertation). Lubbock, TX: Texas Tech. University.
- Spaeth, K. E., Peacock, G. L., Herrick, J., Shaver, E. P., & Dayton, R. (2005). Current and future applications of the USDA-NRCS rangeland NRI. *Journal of Soil Water Conservation*, 60(5), 114A.
- Spaeth, K. E., Pierson, F. B., Herrick, J. E., Shaver, P. L., Pyke, D. A., Pellant, M., . . . Dayton, B. (2003). New proposed national resources inventory protocols on nonfederal rangelands. *Journal of Soil Water Conservation*, 58(1), 18A–21A.
- Spaeth, K. E., Pierson, F. B., Wertz, M. A., & Awang, J. B. (1996). Gradient analysis of infiltration and environmental variables as related to rangeland vegetation. *Transactions of the ASAE*, 39(1), 67–77.
- Stone, J. J., Lane, L. J., & Shirley, E. D. (1992). Infiltration and runoff simulation on a plane. *Transactions of the ASAE*, 35(1), 161–170.
- Stone, J. J., Lane, L. J., Shirley, E. D., & Hernandez, M. (1995). Hillslope surface hydrology, In D. C. Flanagan & M. A. Nearing (Eds.), *USDA-Water Erosion Prediction Project (WEPP), Hillslope Profile and Watershed Model Documentation Technical Documentation* (NSERL Rep. 10, Chapter 4, pp. 4.1–4.20). West Lafayette, IN: USDA-ARS National Soil Erosion Research Laboratory.
- Swanson, N. P. (1965). Rotating-boom rainfall simulator. *Transactions of the ASAE*, 8(1), 71–72.
- Thompson, S. E., Harman, C. J., Heine, P., & Katul, G. G. (2010). Vegetation-infiltration relationships across climatic and soil type gradient. *Journal of the Geophysical Research*, 115, G02023. <https://doi.org/10.1029/2009JG001134>
- Tromble, J. M., Renard, K. G., & Thatcher, A. P. (1974). Infiltration for three rangeland soil-vegetation complexes. *Journal of Range Management*, 27(4), 318–321.
- Turnbull, L., Wilcox, B. P., Belnap, J., Ravi, S., D'odorico, P., Childers, D., . . . Sankey, T. (2012). Understanding the role of ecohydrological feedbacks in ecosystem state change in drylands. *Ecohydrology*, 5, 174–183.
- United Nations Convention to Combat Desertification (UNCCD) (1994). *United Nations Convention to combat desertification in countries experiencing serious drought and/or desertification, particularly in Africa, Homepage UNCCD*. Retrieved from www.unccd.int
- United States Department of Agriculture (USDA) (2014). *National Resources Inventory, USDA-NRCS handbook of instructions for rangeland field study data collection*. Washington, DC.
- Urguehe, A. M., & Bautista, S. (2015). Size and connectivity of upslope runoff-source areas modulate the performance of woody plants in Mediterranean drylands. *Ecohydrology*, 8, 1292–1303.
- Wainwright, J., Parsons, A. J., & Abrahams, A. D. (2000). Plot-scale studies of vegetation, overland flow and erosion interactions: Case studies from Arizona and New Mexico. *Hydrological Processes*, 14, 2921–2943.
- Wei, H., Nearing, M. A., Stone, J. J., Guertin, D. P., Spaeth, K. E., Pierson, F. B., Nichols, M. H., & Moffett, C. A. (2009). A new splash and sheet erosion equation for rangelands. *Soil Science Society of America Journal*, 73, 1386–1392.

- Weltz, M. A., Kidwell, M. R., & Fox, H. D. (1998). Influence of abiotic and biotic factors in measuring and modeling soil erosion on rangelands: State of knowledge. *Journal of Range Management*, 51(5), 482–495.
- Weltz, M. A., Jolley, L. W., Hernandez, M., Spaeth, K. E., Rossi, C., Talbot, C., . . . Morris, C. (2014a). Estimating conservation needs for rangelands using National Inventory Assessments. *Transaction of the ASABE*, 57(6), 1559–1570.
- Weltz, M. A., Ritchie, J. C., & Fox, H. D. (1994). Comparison of laser and field measurements of vegetation height and canopy cover. *Water Resources Research*, 30(5), 1311–1319.
- Weltz, M. A., Speath, K. E., Taylor, M. H., Rollins, K., Pierson, F. B., Jolley, L. W., . . . Rossi, C. (2014b). Cheatgrass invasion and woody species encroachment in the Great Basin: Benefits of conservation. *Journal of Soil and Water Conservation*, 69(2), 39A–44A.
- West, N. E. (1991). Nutrient cycling in soils of semiarid and arid regions. In J. Skujins (Ed.) *Semiarid lands and deserts: Soil resource and reclamation* (pp. 295–332). New York, NY: Marcel-Dekker.
- Wilcox, B. P., Breshears, D. D., & Allen, C. D. (2003). Ecohydrology of a resource-conserving semiarid woodland: Effects of scale and disturbance. *Ecological Monographs*, 73(2), 223–239.
- Wilcox, B. P., Pitlick, J., Allen, C. D., & Davenport, D. W. (1996). Runoff and erosion from a rapidly eroding pinyon-juniper hillslope. In M. G. Anderson & S. M. Brooks (Eds.), *Advances in hillslope processes* (pp. 61–71). New York, NY: John Wiley.
- Wilcox, B. P., Seyfried, M. S., Breshears, D. D., & McDonnell, J. J. (2012). Ecohydrologic connections and complexities in drylands: New perspectives for understanding transformative landscape change. *Ecohydrology*, 5, 143–144.
- Williams, C. J., Pierson, F. B., Al-Hamdan, O. Z., Kormos, P. R., Hardegree, S. P., & Clark, P. E. (2014a). Can wildfire serve as an ecohydrologic threshold-reversal mechanism on juniper-encroached shrublands. *Ecohydrology*, 7, 453–477.
- Williams, C. J., Pierson, F. B., Robichaud, P. R., Al-Hamdan, O. Z., Boll, J., & Strand, E. K. (2016a). Structural and functional connectivity as a driver of hillslope erosion following disturbance. *International Journal of Wildland Fire*, 25, 306–321.
- Williams, C. J., Pierson, F. B., Robichaud, P. R., & Boll, J. (2014b). Hydrologic and erosion responses to wildfire along the rangeland-xeric forest continuum in the western US: A review and model of hydrologic vulnerability. *International Journal of Wildland Fire*, 23, 155–172.
- Williams, C. J., Pierson, F. B., Spaeth, K. E., Brown, J. R., Al-Hamdan, O. Z., Weltz, M. A., . . . Nichols, M. H. (2016b). Incorporating hydrologic data and ecohydrologic relationships into ecological site descriptions. *Ecology & Management*, 69, 4–19. <http://doi.org/10.1016/j.rama.2015.10.001>
- Woolhiser, D. A., Smith, R. E., & Goodrich, D. C. (1990). *KINEROS, a kinematic runoff and erosion model: Documentation and user manual* (ARS-77, 130 pp.). Tucson, AZ: U.S. Department of Agriculture, Agricultural Research Service.
- Yalin, Y. S. (1963). An expression for bed-load transportation. *Journal of Hydraulics Division ASCE*, 89(HY3), 221–250.
- Zhang, X. C., Nearing, M. A., & Risse, L. M. (1995). Estimation of Green-Ampt conductivity parameters: Part I. Row crops. *Transactions of the ASAE*, 38(4), 1069–1077.